This is the Pre-Published Version.
X. Zhang, X. Wu, Y. Park, X. Huang, T. Zhang, F. Xiao, A. Usmani (2021) *Perspectives of Big Experimental Database and Artificial Intelligence in Tunnel Fire Research*, **Tunn. Undergr. Space Technol.**, 108, 103691. doi: 10.1016/j.tust.2020.103691

Perspectives of Big Experimental Database and Artificial Intelligence in Tunnel Fire Research

Xiaoning Zhang[1,2], Xiqiang Wu[1,*], Younggi Park[1], Tianhang Zhang[1], Xinyan Huang[1,*], Fu Xiao[1], Asif Usmani[1,2]

[1]*Department of Building Services Engineering, Hong Kong Polytechnic University*

[2]*Research Institute for Sustainable Urban Development, Hong Kong Polytechnic University*

Highlights

- Review the history, methods, and key parameters of tunnel fire research.
- Establish an experimental database of full-scale and model-scale tunnel fire tests.
- Database is open access online and available for updating by the fire community.
- Application of machine learning and experimental database to predict tunnel fire.

Abstract: Tunnel fire is one of the most severe global fire hazards and causes a significant amount of economic losses and casualties every year. Over the last 50 years, numerous full-scale and reduced-scale tunnel fire tests, as well as numerical simulations have been conducted to quantify the critical fire events and key parameters to guide the fire safety design of the tunnel. In light of the recent advances in big data and artificial intelligence, this paper aims to establish a database that contains all existing experimental data of tunnel fire, based on an extensive literature review on tunnel fire tests. This tunnel-fire database summarizes seven key parameters of flame, ventilation, and smoke in a GitHub site: https://github.com/PolyUFire/Tunnel_Fire_Database. The test conditions, experimental phenomena, and data of each literature work were organized and categorized in a standard format that could be conveniently accessed and continuously updated. Based on this database, machine learning is applied to predict the critical ventilation velocity of a tunnel fire as a demonstration. The review of the current database not only reveals more valuable information and hidden problems in the conventional collection of test data, but also provides new directions in future tunnel fire research. The established database and methodology help promote the application of artificial intelligence and smart firefighting in tunnel fire safety.

Keywords: big data; empirical model; deep learning; critical event; smart firefighting

Graphic Abstract

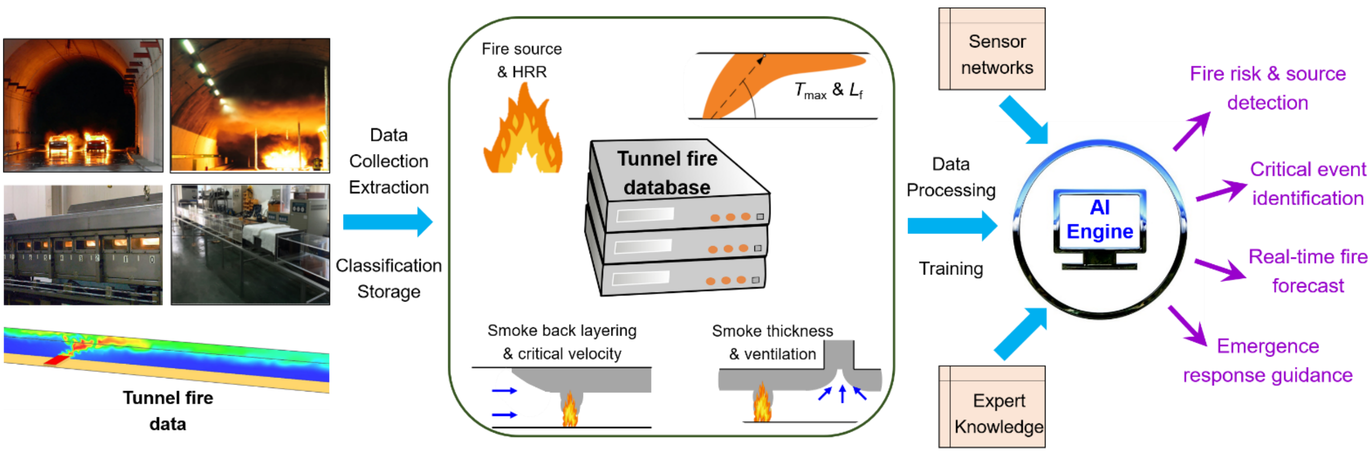

Nomenclature

Symbols		***Greeks***	
A	cross-section area (m^2)	ρ	density (kg/m^3)
A_s	aspect ratio, H/w (-)	k	turbulence energy (m^2/s^2)
b	equivalent radius of fire source (m)	$\alpha, \gamma, \varepsilon$	experimental constants
b_f	radius of the fire source (m)	β	percentage of the tunnel slope
c_p	specific heat of air (kJ/kg-K)	φ	blockage ratio
d_s	thickness of smoke layer (m)		
D_H	hydraulic diameter (m)	***Superscripts***	
D	fire source diameter (m)	*	dimensionless parameter
Fr	Froude number		
g	gravitational acceleration (m/s^2)	**Subscripts**	
h_{sm}	smoke layer height (m)	a	ambient or air
H	height (m)	c	critical
ΔH	heat of reaction (MJ/kg)	ef	effective
$\bar{H}$	hydraulic diameter of tunnel (m)	f	flame
I	integration of equation	F	full scale
K	fitting constant	g	gas
l	flame length (m)	i	smoke layer interface
L_b	back-layering distance (m)	l	lower
$L*$	dimensionless backlayering length	max	maximum
L_f	flame length (m)	M	model scale
$\dot{m}$	mass flow rate (kg/s)	r	radiation
N	value in the N-percentage rule	sm	smoke
N_L	value of buoyancy frequency (s^{-1})	sh	shaft
$\dot{q}''$	heat flux (kW/m^2)	u	upper
$\dot{Q}$	heat release rate (MW)		
Q'	heat release rate per unit length (kW/m)	**Abbreviation**	
$\dot{Q}^*$	dimensionless heat release rate (-)	*AI*	artificial intelligence
$\dot{Q}_c$	convective heat release rate (MW)	*CFD*	computational fluid dynamics
r	radial distance (m)	*CNN*	convolutional neural network
Ri	Richardson number (-)	*CVV*	critical ventilation velocity
Ri'	modified Richardson number (-)	*FDS*	fire dynamics simulator
Re	Reynolds number (-)	*FFFS*	fixed fire fighting system
t	time (s)	*HGV*	heavy goods vehicle
T	temperature (K)	*HRR*	heat release rate (MW)
T_i	smoke layer interface temperature (K)	*LPG*	liquefied petroleum gas
T_{max}	maximum ceiling temperature (K)	*LSTM*	long short-term memory
ΔT	temperature difference (K)	*MSE*	mean squared error
v	velocity (m/s)	*NVS*	natural ventilation system
V	ventilation velocity (m/s)	*OD*	optical density (-)
V^*	dimensionless ventilation velocity	*pHRR*	peak heat release rate (MW)
w	width of tunnel (m)	*RNN*	recurrent neural network
z	vertical height (m)	*SVM*	support vector machines
z_0	virtual origin height (m)	*TCNN*	transpose convolutional neural network
		TST	Tunnel Safety Test

1. Introduction

Tunnels have played an essential role in modern transportation systems since the mid-20th century, owing to their high utility and flexibility in mountainous areas and their effectiveness in tackling the tight land supply of crowded metropolitan areas. However, as a significant infrastructure hazard, fires in tunnels cause a great deal of economic and social losses each year (Beard and Carvel, 2012; Carvel, 2019; Casey, 2020; Ingason *et al*., 2015a; Li and Liu, 2020).

Fig. 1 shows some recent severe tunnel fire accidents. For instance, two trucks collided in 2001 at the Gottard Road Tunnel in Switzerland, causing a fire in the tunnel (Fig. 1a). Since then, new fire regulations limit the number of trucks inside the tunnel. In 2008, a fire occurred to a heavy goods vehicle (HGV) in the Channel tunnel of the France side. The fire quickly spread from the burning truck to the next 6 cars (Fig. 1b). The firefighting lasted for around 16 hours, and many people were injured due to the smoke inhalation. In 2014, a coal truck collided with a methanol-tanker truck inside the Yanhou Tunnel, China. The liquid methanol flame triggered a rapid fire spread and a series of explosions, causing more than 30 deaths (Fig. 1c). Statistics showed there had been 161 medium and large tunnel fire accidents in China from 2000 to 2016 (Ren *et al*., 2019). In 2015, an oil tank truck hit the wall inside Skatestraum tunnel, Norway, sparking about 16,500 L gasoline, and the fire fast spread over 500 meters. Despite no major injuries, the tunnel wall was severely damaged (Fig. 1d). In 2019, a fire broke out in a single medium-sized car at Rannersdorf tunnel, Austria, due to vehicle defects (Fig. 1e). In 2020, a fire accident occurred in the Samae 2 Tunnel, Korea, where dozens of tanks and trucks collided, killing four people and injuring more than 40 others (Fig. 1f). The damage was severe because of no scraper and ventilation system.

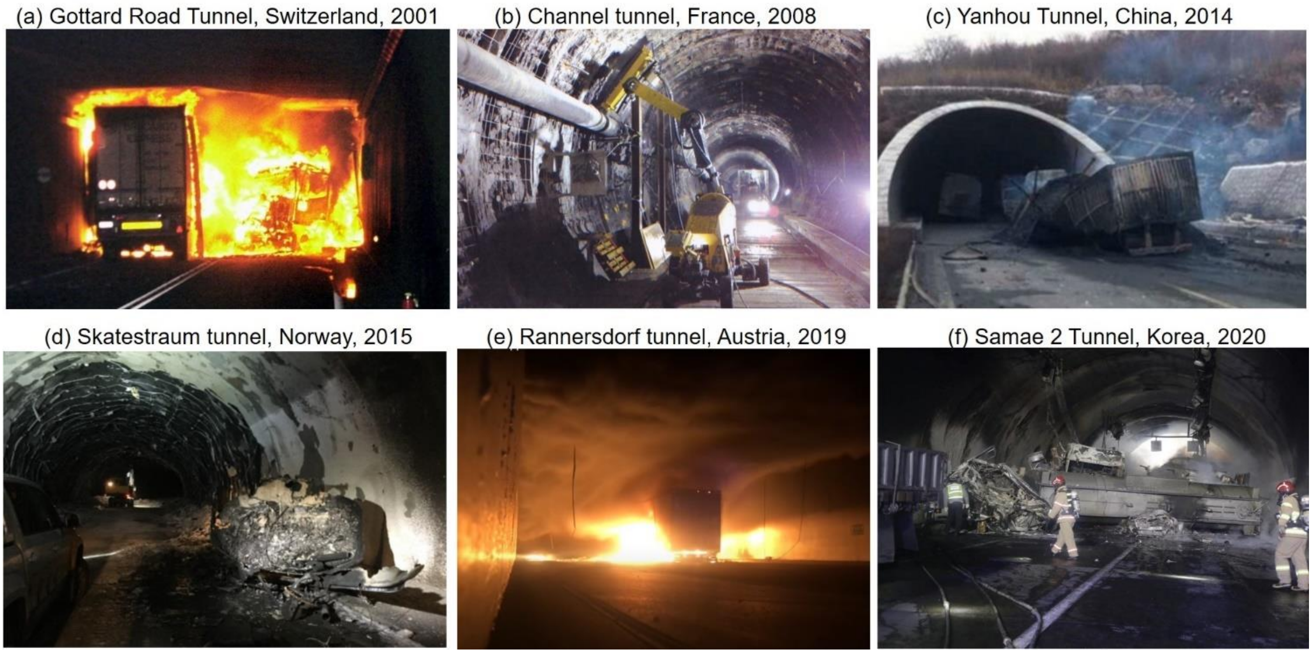

Fig. 1. Recent tunnels after fire accidents.

Table 1 further lists some major fire accidents that took place inside the tunnel with severe casualties over the last 50 years, and more detailed database of tunnel fire accidents are available online with continuous updates https://github.com/PolyUFire/Tunnel_Fire_Database. Despite continuous researches and improved fire safety regulations for modern road and rail tunnels, disastrous fire accidents continue breaking out all over the world. In many tunnel fires, the structural integrity of the tunnel was severely damaged due to the long-lasting fire thermal impact, as shown in Fig. 1. The frequent occurrence of tunnel fires around the world re-emphasizes the importance of the tunnel fire safety design, early detection, and the initial fire suppression. In the event of a tunnel fire accident, to prompt a safe evacuation, initial suppression is the most important thing, due to the fast fire development and limited regress time. Many studies have been carried out on the optimization of tunnel design to mitigate the impact of the fire hazard. For tunnels, early detection of fire is a cost-effective way to prevent fires from developing into a potentially catastrophic event. It is also important to identify the real-time fire scenarios, and predict the fire evolution based on toxic substances, and flame propagation in various scenarios by using fire detectors, sensors, and other more advanced methods.

Table 1. Selected major tunnel fire accidents with severe casualties over the last 50 years (Casey, 2020; Ingason et al., 2015a; Ren et al., 2019; Vianello et al., 2012).

Year	Tunnel Location	Accident type	Casualties	Comments
1972	Hokuriku tunnel, Japan	short circuit	744	No extinguisher, no smoke exhaust system
1976	Crossing BP - A6, France	Lorry fire	12	Serious damage over 150 m
1978	Velsen tunnel, Nederland	Collision	10	Serious damage over 30 m
1979	Nihonzaka Tunnel, Japan	Collision	8	Serious damage over 1,100 m
1980	Sakai, Japan	Collision	10	Serious damage to structure
1982	Caldecott, USA	Collision	9	Serious damage over 580 m
1983	Pecrile, Italy	Collision	31	-
1984	San Benedetto tunnel, Italy	Bomb attack	137	Railway tunnel
1986	L'Arme, France	Collision	8	-
1993	Serra Ripoli Tunnel, Italy	Collision	8	-
1993	Hovden, Norway	Collision	5	111 m insulation material destroyed
1994	Hugouenot, South Africa	Electrical fault	29	Serious damage on tunnel lining
1995	Pfander Tunnel, Austria	Collision	7	Serious damage to structure
1995	Baku underground railway, Azerbaijan	Electrical malfunction	559	-
1996	Channel Tunnel, Britain-France	Cargo fire	-	Widespread damage on tunnel region
1996	Isola delle Femmine, Italy	Collision	25	Serious damage to tunnel, closed for 2.5 days
1999	Mont Blanc, France-Italy	Oil leakage Motor	39	Serious spalling on tunnel lining
1999	Tauren Tunnel, Austria	Multi-car collision	61	Part of tunnel vault collapsed
2000	Seljestad tunnel, Norway	Multi-car collision	6	Structural damage and closed for 1.5 days
2000	Gletscherbahn Kaprun, Austria	Electric fan heater	155	Fire had burned through a 16-kW power cable
2001	Gothard, Switzerland	Collision of two trucks	21	Serious spalling on tunnel lining
2001	Gleinalm tunnel, Austria	Collision	9	Tunnel structures seriously damaged
2001	Prapontin tunnel, Italy	Self-ignition of tire	11	-
2001	Madaoling Tunnel, China	Engine fire	18	-
2003	Vicenza, Italy	Bus turnover	56	-
2003	Daegu subway, South Korea	Subway fire	340	Rapid spread of flames and smoke due to petrol incendiary incidents
2003	Baregg Tunnel, Switzerland	Collision	6	-
2004	Takayama, Japan	Collision	5	Surface concrete damage
2005	Frejus, France-Italy	Car accident	23	Serious damage on tunnel lining
2005	Feiluanling tunnel, China	Passenger car brake failure	8	-
2006	Viamala, Switzerland	Car-bus collision	15	-
2007	San martino, Italy	Collision	12	-
2007	Chongqing Univ. tunnel, China	Technical problems	6	Lighting and ventilation system are paralyzed
2007	Newhall Pass tunnel, USA	Multi-truck collision	13	It took 24 hours to control the fire, and structure was severely damaged
2008	Ofenauer, Austria	Collision	17	-
2009	Gubrist, Switzerland	Collision	4	-
2009	Eiksund Tunnel, Norway	Collision	5	-
2010	Huishan Tunnel, China	Man-made arson	43	Damage on mechanical and electrical facilities
2012	Xueshan Tunnel, China	Collision	24	-
2013	Liushiliang Tunnel, China	Multi-car collision	18	Damage on tunnel facilities
2014	Yanhou, China	Collision	31	Serious damage on tunnel lining
2017	Taojiakuang tunnel, China	Arson	11	-
2019	Maoliling Tunnel, China	Self-ignition of tire	36	-
2020	Central Park North–110th Street station, USA	Possible arson	17	Severe damages in the station and the train cars
2020	Samae 2 Tunnel, Korea	Collision	47	Tank truck carrying nitric acid ran into some cars involved in an earlier accident

1.1. Tunnel fire research

From the mid-19th century, early researchers had noticed the disastrous influence of tunnel fire and the importance of securing evacuation safety. Later, statistics further confirmed that most casualties of tunnel fire were induced by smoke inhalation (Beard, 2009), which is similar to the residential fire accidents. However, not many tunnel fire tests were done. It is because, with limited understanding of fire science, it is difficult to guarantee researchers' life safety in the large-scale fire test. By the 1950s, studies on tunnel fire were still limited and mainly focused on construction safety (ANDERSON, 1936), ventilation systems (Ole and Cruthers, 1947), and fire protection systems (Sevcik, 1928). Since then, more and more fire research have been conducted in tunnels of different scales, and new tunnel fire safety codes have been applied to alleviate and limit the threats of toxic gases and smoke (Carvel, 2019). For all these studies, the most important issue is the efficiency of the Fixed Fire Fighting System (FFFS), particularly the ventilation system, that ensures the safety of evacuees.

In general, a typical tunnel fire research adopts three approaches, namely, full-scale fire test in a real tunnel, reduced-scale test in the laboratory, and numerical simulation based on computational fluid dynamics (CFD). The results of full-scale tunnel fire tests are considered as most reliable and valuable, which are used to verify the results of reduced scale fire tests or guide the tunnel fire-safety design. Some well-known full-scale tests include the EUREKA EU499 tests (Norway, 1990-92) (Haack, 1998), Memorial tunnel tests (USA, 1993–95) (Giblin, 1997), and METRO tests (Sweden, 2009-12) (Ingason *et al*., 2012). However, real-scale tests are costly and dangerous, so to date, full-scale tunnel fire test data are still quite limited (Ingason *et al*., 2015a). On the other hand, the model-scale or reduced-scale laboratory tests, based on the scaling laws, provide a greater number of experimental data (Ingason and Zhen, 2010). In addition to the conventional studies on smoke motion, model-scale tests have also been used to evaluate the performance of the water spray system and the evacuation model (Ingason and Zhen, 2010; Li and Ingason, 2013).

With the recent improvement of the computational capacity, the CFD simulations techniques have been more widely applied in tunnel fire research and tunnel fire safety design, like other fire research areas. The most popular CFD tool is the Fire Dynamics Simulator (FDS) (McGrattan *et al*., 2019) developed by National Institute of Standards and Technology (NIST). The numerical simulations can potentially provide much more information that is difficult to measure in experiments. In fact, combining the experiments of various scales and numerical simulations has become a common approach in recent tunnel fire researches (Li et al., 2012; Weng et al., 2015), as well as the performance-based design for tunnel fire safety (Ingason *et al*., 2015a; Meacham *et al*., 2005). The tunnel fire research has also helped develop the development the international standards (AIPCR, 1999; Bendelius *et al*., 2007; Egger, 2001; NFPA, 2014, 2011) and handbooks (Blennemann and Girnau, 2005; Cote, 2008; Kennedy, 1976; Kuesel *et al*., 2012) related to tunnel fire safety, such as NFPA 130 and NFPA 502. Many other countries have also developed their own regulations or guidelines, such as Japan (Japan Road Association, 1985).

However, many tunnel-fire problems remain that need further research, like the early detection, emergency evacuation, and the prediction of tunnel fire behaviors. Once a fire occurs in the tunnel, the real-time information on site like fire location and size, as well as the location and number of people, are essential for the firefighting and the emergency decision making. Various fire detection technologies have been adopted for tunnel fire engineering. Although existing techniques such as a line-type heat detectors and cameras can locate the fire, these techniques become invalid in a short time due to the rapid development fire and smoke transport, and their installation and maintenance costs are too high (Jevtić and Blagojević, 2014). Therefore, besides preventing the tunnel fire, smart fire detection, and real-time forecast capability will play a central role in future research.

1.2. Big data and AI on fire research

The concept of artificial intelligence (AI) was initially proposed on a workshop held in Dartmouth College in 1956 for dealing with computational problems related to language understanding, storage of data, and pattern matching (Russell and Norvig, 2016). Since then, AI approaches, as well as other cutting-edge technologies such as remote monitoring, high-resolution sensor, high-speed computation, data-driven methods have been increasingly applied in fire safety engineering (Grant *et al*., 2015). For example, Choi *et al*. (2016) proposed a data-driven system for detecting flame with a virtual camera, which showed a high accuracy using a nonlinear classifier. Deep learning models imitating the human brain, including convolutional neural networks (CNNs) and recurrent neural networks (RNNs) have been proposed by researchers (Jaafari *et al*., 2019; Mahdevari and Torabi, 2012). Compared with conventional AI and machine-learning models, deep learning models require more data to automatically learn hidden features from the massive data.

In fire engineering, deep learning algorithms with big data and high-speed computation have also been adopted in tunnel fire and compartment fire. For example, Hodges *et al.* (2018;2019) used transpose convolutional neural network (TCNN) and simulating results conducted by FDS to predict the temperature distribution inside compartment rooms. Ghoreishi (2019) compared the performance of various models and demonstrated the feasibility of their faster regional CNNs in detecting fire, meanwhile limiting the false positive. Cao *et al.* (2019) proposed an enhanced bidirectional LSTM model to predict wildland fire with video images. It was reported that this method could provide more accurate prediction since it can take tempo-spatial features into account to detect fire. These studies explored the potential application of AI methods in the detection and forecasting of fire (Kim et al., 2019; Mahdevari and Torabi, 2012; Naser, 2019; Wu et al., 2020a).

However, all AI models need to be fine-tuned before being applied to practical problems. Often this is realized through sufficient training iterations on a database containing a large volume of data. A well-structured database is thus inevitable for the training of the AI models. The establishment of the database could be a challenging task since a sufficient amount of data need to be extracted from previous works, and then these data should be organized in a format to be conveniently used for further training. Besides, this task requires expertise knowledge knowing the important factors related to tunnel fire, such as the fire size, ventilation type and fan performance, burning material. For example, Naser *et al*. (2019) built up a database by collecting large amounts of data on material components of timber structures and correlated equations derived from fire tests. The fire resistance of timber structures was predicted by an AI model and the established database. For tunnel fires, Wu *et al*. (2020a; 2020b) established a big tunnel-fire database of numerical simulations for varying fire locations and sizes, and ventilation conditions, and then demonstrated the use of AI and deep learning to identify the fire source and forecast the temperature field and evolution of tunnel fire.

To date, though tunnel fire research have been well reviewed by top researchers (Barbato et al., 2014; Carvel, 2019; Casey, 2020; Li and Ingason, 2018; Ntzeremes and Kirytopoulos, 2019; Pei and Zhang, 2019; Singh and Khurana, 2019), most of these reviews did not extract test results to form a standardized database that can be accessed freely and easily. Other researchers still have no choice but to repeatedly devote massive time and energy to developing their own databases and analysis. Compared with experimental data, numerical data could not only be too massive to present and analyze, but also questionable before careful verifications. Thus, a database containing sufficient and precious experimental data would be most useful and preferable for AI applications and smart firefighting.

This paper targets to establish a comprehensive experimental database on tunnel fire specialized for the application of AI algorithms. Section 2 reviewed the available sources of experimental results on multi-scaled tunnel fire tests. Section 3 classified these studies into several critical parameters in tunnel fire, including flame characteristics, ventilation, smoke layer conditions, and so on. Then, experimental data or empirical correlations were extracted and organized in a consistent manner. Afterward, a demonstration was given in Section 4 to vividly illustrate how to train an AI model with the established experimental database to predict the critical velocity of tunnel fires.

2. Overview of tunnel fire tests

2.1. Real-scale test and data

It is challenging to conduct real-scale (or full-scale) fire tests in a real tunnel, because of their high cost, safety concerns, and environmental issues. Nevertheless, the limited number of real-scale experiments have already made a great contribution to the understanding of tunnel fire, because they are most close to the real tunnel-fire accidents and can form the foundation for other small-scale experiments and numerical simulations. Fig. 2 shows several recent full-scale fire tests in actual tunnels and the road map of these valuable tests. Table 2 summarizes the information on these tests, including tunnel conditions and goals. More detailed descriptions can be found in (Beard and Carvel, 2012). These tests aim to ensure safe evacuation in case of tunnel fire, and most emphasized on the FFFS, such as ventilation system and sprinklers, that operated in fire incidents. It is worth noting that full-scale fire tests are not perfect in practice, but restricted by many factors, such as the geometry and shape, as well as the fire protection systems, i.e., less flexible. As these parameters are essentially fixed for a given test tunnel, it is difficult to examine them in a real-scale tunnel fire test.

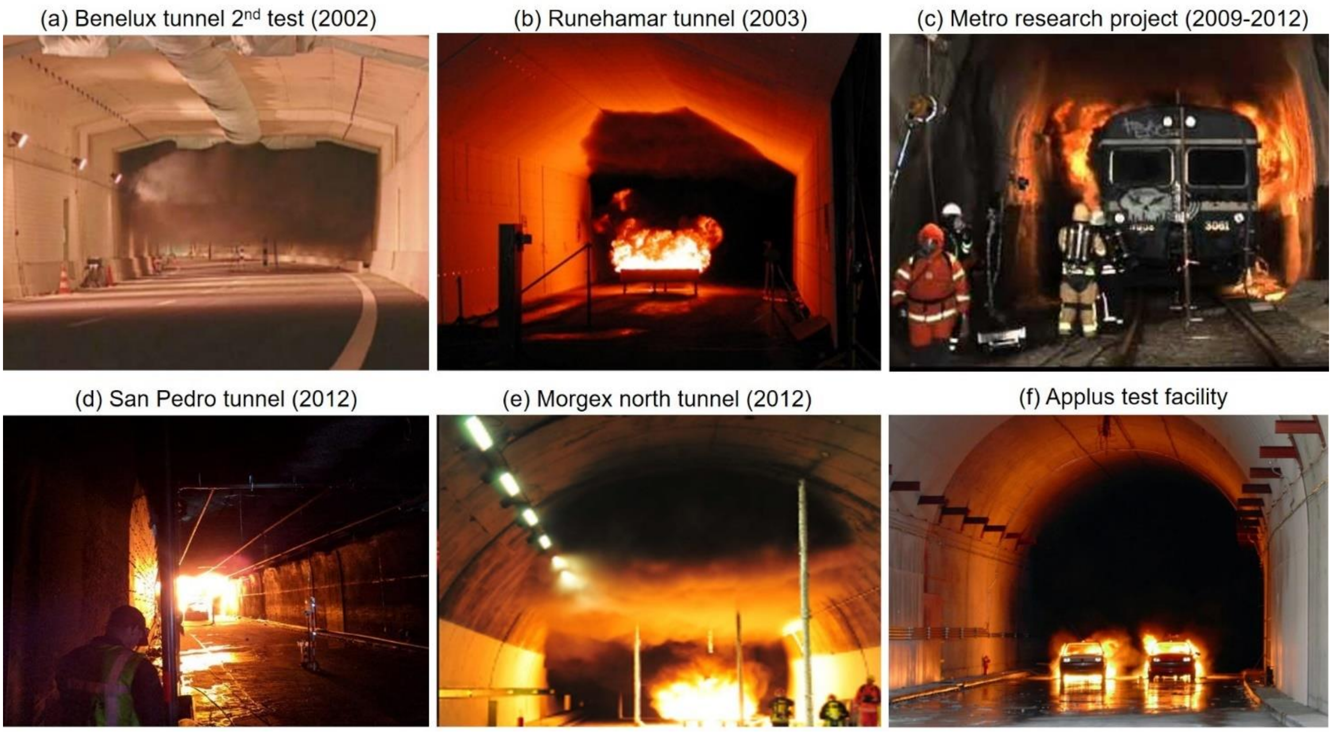

Fig. 2. Real-scale tunnel fire tests and facilities, (a) Benelux tunnel 2nd test in 2002, (b) Runehamar tunnel in 2003 (Ingason *et al*., 2015b), (c) Metro research project from 2009 to 2012, (d) San Pedro tunnel in 2012, (e) Morgex north tunnel in 2012, and (f) Applus test facility.

In terms of experimental data, although it is almost impossible to directly obtain the on-site measurements of carbon monoxide, carbon dioxide, and temperature distribution of fire in the existing tunnels, the information of tunnel dimension, fire source location, and the heat release rate (HRR) can still be collected. In particular, the HRR was measured in almost all experiments, because other fire information, such as flame temperatures and height, can be easily derived from the HRR. The factors influencing the transient HRR and the maximum HRR, including fire size and ventilation conditions, attracted extensive studies. It is also worth noting that HRR is also regarded as a key factor for performance-based design. Apart from the HRR, most of existing tunnel-fire tests were also conducted for the purpose of studying the smoke transport and control, as smoke is the leading cause of casualties. To alleviate the tunnel fire hazard, fire suppression systems are generally designed and installed in tunnels (Ingason et al., 2015a). Table 2 also listed the real-scale tunnel fire tests on fire suppression systems, such as sprinklers and fire extinguishers, under different fire scenarios.

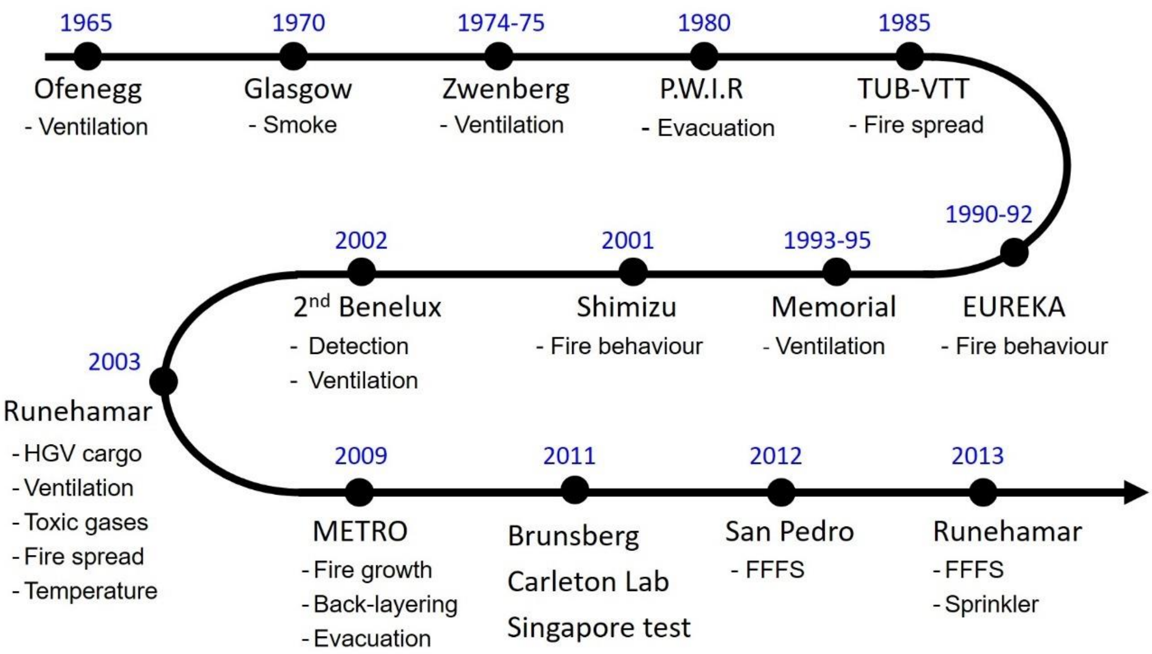

Fig. 3. Footprints of real-scale tunnel fire experiments with year, name, and major test parameters.

Recent full-scale tunnel fire tests have served as the core data for both theoretical and numerical analyses (Hu *et al*., 2006; Liu *et al*., 2017), which presented the distribution of ceiling temperature in tunnels under a natural ventilation system. The temperature distributions in horizontal and vertical directions were suggested to be correlated with dimensionless coefficients. For example, the decay of temperature in the longitudinal direction could be correlated with the dimensionless HRR (Q^*) and fire locations. Ji *et al.* (2010) analyzed the effect of smoke vent height and exhaust velocity on mechanical ventilation. The phenomenon of plug-holing under the natural ventilation system is rarely studied. Hinkley (1970) proposed a formula for the analysis of the occurrence of the plug-holing phenomena (see Section 3.7). Currently, we are still unclear about the boundary layer for the mixture of fresh air and smoke, which often occurs in the vertical shaft area where only limited devices are available.

These real-scale tunnel fire tests demonstrated the important effects of fan position and wind speed on fire spread, temperature distribution, smoke distribution, and evacuation strategies. So far, researches have made lots of efforts to investigate the fundamental fire parameters, such as HRR, temperature distributions (Hu *et al*., 2006; Liu *et al*., 2017; Wang *et al*., 2016, 2015), ventilation performances (Feng *et al*., 2020; Yu *et al*., 2018; Zhou *et al*., 2019), and wind (Węgrzyński and Lipecki, 2018). Some of these results are listed in Table 3. detailed in Section 3. However, only limited studies have addressed more complex tunnel fire phenomena, including plug-holing (Jie *et al*., 2010) and back-layering (Hu *et al*., 2008), because these parameters are more difficult to quantify a real-scale tunnel. In short, more tunnel-fire tests are needed in future research to quantify the influence of the type of tunnels and fans on these complicated fire phenomena.

Table 2. Summarization of results on real-scale experiments

<table>
<tr><th>Test program, country, year</th><th>Length [m]</th><th>Height [m]</th><th>A [m²]</th><th>Fire source</th><th>pHRR [MW]</th><th>No. of tests</th><th>Measurements</th><th>Comments</th></tr>
<tr><td rowspan="2">Ofenegg, Switzerland, 1965 (Ingason et al., 2015a)</td><td>190</td><td>6</td><td>23</td><td>Gasoline (6.6, 47.5, 95 m^2)</td><td>11-80</td><td>11</td><td>T, CO, O_2, visibility</td><td>Single trail tunnel, dead end, sprinkler</td></tr>
<tr><td colspan="8">Main purpose: Investigating the ventilation capacities depending on types of ventilation such as natural, longitudinal, and semi-transverse.
Main implication and conclusion: Results proved the importance of using deluge sprinkler nozzles in Europe</td></tr>
<tr><td rowspan="2">Glasgow, UK 1970 (Heselden and Hinkley, 1970)</td><td>620</td><td>5.2</td><td>39.5</td><td>Kerosene (1.44, 2.88, 5.76 m^2)</td><td>2-8</td><td>5</td><td>T, OD</td><td>Disused railway tunnel</td></tr>
<tr><td colspan="8">Main purpose: Investigating smoke spread in an enclosed shopping mall. Main conclusion: Smoke layers were distributed horizontally.</td></tr>
<tr><td rowspan="2">Zwenberg, Australia, 1974-75 (Ingason et al., 2015a)</td><td>390</td><td>3.9</td><td>20</td><td>Gasoline (6.8, 13.6 m^2)
wood, and rubber</td><td>8-21</td><td>30</td><td>T, CO, CO_2, NOx, CH, O_2, v, OD</td><td>Disused railway tunnel</td></tr>
<tr><td colspan="8">Main purpose: Investigating the effects of different types of ventilation on the smoke spreading, heat and toxic gases considering evacuees.
Main conclusion: (1) Ventilation systems beyond adequate capacity exacerbated the distribution of smoke and damage areas; (2) Longitudinal ventilation should be shut down to hinder the introducing of longitudinal flow; and (3) Results have become a guidance of designing ventilation systems around the world.</td></tr>
<tr><td rowspan="2">P.W.R.I, Japan, 1980 (Ingason, 2006)</td><td>700</td><td>~6.8</td><td>57.3</td><td>Gasoline (4, 6 m^2), 9-14 passenger car, bus</td><td>-</td><td>16</td><td>T, CO, CO_2, v, OD, $\dot{q}_r''$</td><td>Special test tunnel, sprinkler</td></tr>
<tr><td colspan="8">Main purpose: Determining the environments for evacuees.
Main conclusions: (1) It is the fact that the wind velocity increased, the smoke spreading throughout whole areas of tunnels affect evacuees perilously; (2) Wind speed to prevent back-layering is 3.5 m/s, but wind speed above that exacerbates the spread of smoke and heat; and (3) Sprinklers can make a precaution.</td></tr>
<tr><td rowspan="2">P.W.R.I, Japan, 1980 (Mashimo, 1993)</td><td>3277</td><td>~6.8</td><td>58</td><td>Gasoline (4 m^2), 9 bus</td><td>-</td><td>8</td><td>T, CO, CO_2, O_2, v, OD, $\dot{q}''$</td><td>In use road tunnel sprinkler</td></tr>
<tr><td colspan="8">Main purpose: Determining the behaviour of smoke and to control smoke and wind velocities considering evacuees.</td></tr>
<tr><td rowspan="2">TUB-VTT, Finland, 1985 (Ingason et al., 2015a)</td><td>140</td><td>5</td><td>24-31</td><td>Wood cribs (simulate subway coach and collision of two cars)</td><td>1.8-8</td><td>2</td><td>HRR, T, m, CO, CO_2, O_2, v, OD</td><td>Disused cavern system</td></tr>
<tr><td colspan="8">Main conclusion: Theoretical calculation from the existing room fire codes did not reliably predict the occurrence of flashover</td></tr>
<tr><td rowspan="2">EUREKA EU499, Norway, 1990-92 (Haack, 1998; Ingason et al., 2015a)</td><td>2300</td><td>4.8-5.5</td><td>25-35</td><td>Wood cribs, heptane pool, cars, metro car, rail cars, HGV trailer</td><td>2-120</td><td>21</td><td>HRR, T, CO, m, CO_2, O_2, SO_2, C_xH_y, NO, visibility, soot, m, v</td><td>Disused transportation tunnel</td></tr>
<tr><td colspan="8">Main purpose: Investigating the fire behavior of different type of fuels including real road and rail vehicles.
Main conclusion: (1) Measuring lots of HRR for real vehicles using the oxygen consumption calorimetry; and (2) the wood crib tests showed a good agreement when increasing fire growth rate while increasing ventilation rate.</td></tr>
<tr><td rowspan="2">Memorial, USA, 1993-95 (Giblin, 1997)</td><td>853</td><td>4.4, 7.9</td><td>36, 60</td><td>Fuel oil (4.5-45 m^2)</td><td>10-100</td><td>98</td><td>HRR, T, CO, CO_2, v, visibility</td><td>Disused road tunnel, sprinkler</td></tr>
<tr><td colspan="8">Main purpose: Investigating the effect of varying types of ventilation system for managing smoke and temperature.
Main conclusions: (1) Ventilation rate for controlling the temperature and smoke spreading cannot be distinguished by considering extraction capabilities. Furthermore, there should be clear criteria for emergency ventilation as it affects ventilation performances; (2) Effects of various ventilation type (full transverse, partial transverse, natural ventilation) were represented; and (3) A huge quantity of oxygen was fired propagation of combustion.</td></tr>
<tr><td>Shimizu No.3, Japan,</td><td>1120</td><td>8.5</td><td>115</td><td>Gasoline (1,4,9 m^2), cars, bus</td><td>2-30</td><td>10</td><td>T, v, OD, $\dot{q}_r''$</td><td>New road tunnel, sprinkler tests</td></tr>
</table>

2001 (Ingason *et al.*, 2015a)	Main purpose: Effect of fire behaviors according to combustion rate, smoke layers, longitudinal flow on the smoke distribution and first of fire spreading. Main conclusion: No huge difference in comparing other real-scale test and effects as, the fire size was too small compared to a large cross-section of a tunnel.							
2nd Benelus tunnel, Netherlands, 2002 (Ingason *et al.*, 2015a)	872	5.1	50	heptane, car, van, HGV mock-up	3-26	14	HRR, T, m, $\dot{q}_r''$, v, OD,	New road tunnel, sprinklers
	Main purpose: Assessing the tenability conditions for escaping, and the efficiency of detections for escaping motorists in the tunnel. Main conclusions: (1) Back-layering of smoke was prevented by 3 m/s for all cases; (2) An open deluge system decreased drastically the temperature profiles; and (3) Deluge sprinkler nozzles reduced gas temperatures significantly, and the magnitude of fire spread was also reduced.							
Runehamar tunnel, Norway 2003 (Ingason *et al.*, 2015b), 2013 (Ingason *et al.*, 2015a)	1600	4.7-5.1	32-47	Cellulose, plastic, furniture, and wood pallets	70-203	4	HRR, T, CO, CO_2, O_2, HCN, H_2O, OD, $\dot{q}_r''$	Disused road tunnel
	Main purpose: Fire spread in HGV cargo loads, effect of longitudinal ventilation, toxic gases, fire spread, firefighting, and temperature development. Main conclusion: (1) Pulsing phenomenon was first observed in the 2003 test; and (2) Early activation of FFFS was able to prevent the fire spreading and reduce the temperature profiles.							
The METRO project, Sweden, 2009-2012 (Ingason *et al.*, 2015a, 2012)	276	~ 6.9	~ 44	Train carriage, and petrol	76-77	-	HRR, T, Smoke, $\dot{q}_r''$, CO, CO_2, O_2,	Real tunnel in Sweden
	Main purpose: Focusing on many parameters; Deigning fires, Evacuation, Fire control, Smoke control, Extraordinary strain, and rescue. Main conclusions: (1) The luggage and open- or closed-door condition are also one of the important factors exacerbating fire development; (2) The design of ventilation system should consider a fast fire growth rate with a peak of 60 MW; (3) Evacuation models should consider the behavior of sequence model, the affiliative model, social influence, and theory of affordances; and (4) Both the pressurizing supply air system and the mechanical exhaust system are effective.							
Brunsberg, Sweden, 2011 (Beard and Carvel, 2012)	276	6.9	44	Metro car	77	2	HRR, T, CO, CO_2, O_2, OD, $\dot{q}_r''$	Disused rail tunnel
	Main purpose: Investigating the effect of fire and combustion materials' spreading in the early stage. Main conclusion: Information of fire spreading, temperature profiles, and HRRs used tor evacuation tests and analysis test.							
Carleton lab, 2011 (Ingason *et al.*, 2015a)	37	5.5	55	Train and subway car	32-55	2	HRR, T, CO, CO_2, O_2	Lab. facility
	Main purpose: Determining the fire development and HRR of a rail car and subway car. Main conclusion: The fire spreading is significantly affected by how many windows were open or air were drawn into the car.							
Singapore test, 2011-12 (Cheong *et al.*, 2014)	600	5.2	37	HGV mock-up	150	7	Nozzle K-factor, HRR, T,	TST tunnel
	Main purpose: Investigating the effect of fire suppression on the HRR and tunnel ventilations, to reduce the risk of vehicular fire spread Main conclusion: Early activation of low-pressure deluge fire system suppression can reduce HRR substantially and significantly affect CO production.							
San Pedro tunnel, Spain, 2012-13 (Ingason *et al.*, 2015a)	600	5.2	37	HGV mock-up	150	1	HRR, T, CO, CO_2, O_2, OD, $\dot{q}_r''$	TST tunnel
	Main purpose: Investigating the effect of Fixed Fire Fighting System (FFFS) such as nozzles, pipes, and pumps. Main conclusions: (1) FFFS plays an important role in reducing HRR, but at the same time it still worked during the firefighting; (2) In the case of diesel pool fires, it showed a tendency to burn up once again to burn diesel remaining in the pool; and (3) The maximum HRR was reached after activation of the FFFS.							

Table 3. Key data of Real- or full-scale tunnel experiments (Feng *et al.*, 2020; F. Guo *et al.*, 2019; Hu *et al.*, 2008, 2006; Liu *et al.*, 2017; Wang *et al.*, 2015; Yu *et al.*, 2018; Zhou *et al.*, 2019).

Reference	Length [m]	Width [m]	Height [m]	D_H [m]	HRR [MW]	$\dot{Q}^*$ [-]	V_c [m/s]	V^* [-]	V_{sm} [m/s]
Guo *et al.* (2019) (Buxton test, 1995)	-	2.74	2.44	238	0.204	0.0059	0.908	0.188	-
					0.606	0.0176	1.438	0.298	
					1.04	0.0303	1.363	0.282	
					1.29	0.0375	1.4	0.290	
					0.57	0.0166	1.037	0.215	
					1.23	0.0358	1.387	0.287	
					0.204	0.0059	0.757	0.157	
Guo *et al.* (2019) (Yuanjiang test, 2006)	-	10.8	7.2	8.4	1.8	0.0088	1.75	0.193	-
					3.2	0.0156	2	0.220	
Guo *et al.* (2019) (Memorial test, 1995)	-	7.6	7.86	7.75	9.3	0.0461	1.85	0.212	-
					13.1	0.0649	2.27	0.26	
					13.9	0.0688	1.92	0.22	
					17.7	0.0877	2.32	0.266	
Liu *et al.* (2017)	1200	5.2	3.4	4.27	-	72-500	-	-	-
Zhou *et al.* (2017b)	600	14	7	9.33	-	-	-	-	0.02-0.65
Hu *et al.* (2008)	1032 (2.1°)	10.8	7.2	-	0.18, 0.32	-	-	-	-
Zhou *et al.* (2019)	600	14	7	-	1	-	-	0.03-025	-
Wang *et al.* (2015)	-	12.35	5.75	2.6	7.5	-	4.65	3.6	-
Yu *et al.* (2018)	2.8 (3.6°)	9	4	-	1, 4	589.6, 2478	-	-	3
Feng *et al.* (2020)	1000	5.4	4.4	-	7.5	-	-	-	2-3.7

2.2. Model-scale experiments and data

As the number of real-scale tunnel fire tests and measured data are limited, the next-best choice is model-scale or reduced-scale experiments (Casey, 2020; Ingason *et al.*, 2015a; Li and Liu, 2020). Because fire tests of smaller scales are easier to conduct, the number of these tests is much larger than that of real-scale tests (see examples in Fig. 4). Through these model-scale tests, the effect of tunnel size and geometry, as well as the fire behaviors, such as the temperature distribution, HRR, and flame height, have been more extensively studied than full-scale tests. Fig. 5 shows a research map categorized by the key research parameters, and Table 4 lists the general information and data of selected model-scale tunnel fire over the last 10 years. Because of the massive amount of model-scale tunnel fire tests, only selected tests with detailed test information are presented, and a more detailed review can be found in (Beard and Carvel, 2012; Beard, 2009; Carvel, 2019; Ingason *et al.*, 2015a; Li and Liu, 2020).

Particularly, the impact of fan type (ventilation conditions), burner location, and tunnel shape on tunnel fire has also attracted much attention. In addition, many fire tests of various scales have been carried out to quantify critical factors related to evacuation, such as the back-layering conditions, e.g. (Q. Guo et al., 2019; Hu et al., 2008; Ingason and Zhen, 2010), ceiling jet flow, e.g. (Cong et al., 2019; Kashef et al., 2013; Oka and Imazeki, 2014a), and critical ventilation velocity (Atkinson and Wu, 1997; Lee and Ryou, 2005; Vauquelin, 2005). In terms of the tunnel firefighting, studies have shown that fire suppression devices (Li et al., 2019; Sarvari and Mazinani, 2019; Sun et al., 2016), such as the sprinkler system, could be affected by obstacles, blockage, and wall construction material, e.g. (Cong et al., 2017; Huang et al., 2019b; Fei Tang et al., 2017a). Undoubtedly, for any fire protection system, it is always a challenge to adequately balance between cost and fire safety issues.

Fig. 4. Examples of model-scale tunnel fire test apparatus (a) 1:40 scale model with varying slope (Lin *et al*., 2019), (b) 1:25 scale model (Chaabat *et al*., 2020), (c) 1:20 scale model with various aspect ratio (Baek *et al*., 2017), (d) 1:13 scale model (Shafee and Yozgatligil, 2018), (e) 1:10 scale model (Gong *et al*., 2016), and (f) 1:5 scale model (Chow *et al*., 2016).

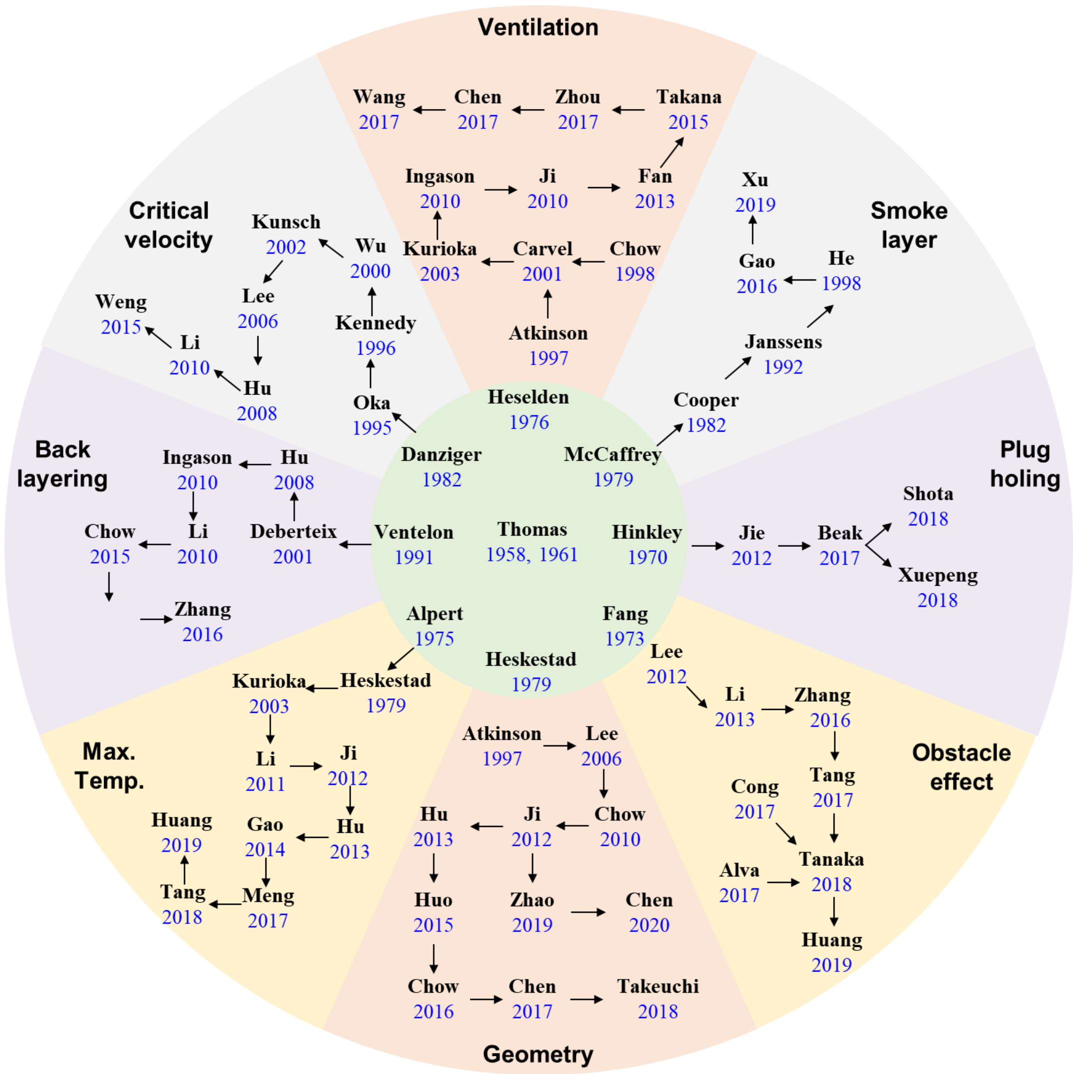

Fig. 5. Footprints of experiments regarding fire itself and tunnels

Table 4. General information and data of selected model-scale tunnel fire over the last 10 years.

Authors/ Projects	Tunnel scale	Length [m]	Height [m]	A [m^2]	Slope [º]	Fire source	HRR [kW]	Ventilation velocity [m/s]	Considered parameter
Oka *et al*. (2010)	-	-	1-1.5	-	5-40	Heptane/ Methanol	9.6/7.3	-	- Response time of a fixed Temp. - Sprinkler, ceiling jet flow
Chow *et al*. (2010)	1:50	-	0.25	0.0665	5-25	Propanol	0.097	-	- Effect of slope on longitudinal ventilation
Li *et al*. (2011)	-	12	5.75	0.0625	-	Propane	4.3 ~ 6	0.05 ~ 0.5	- Temperature, HRR, and Geometry - Longitudinal ventilation
		12	3.93	0.102	-		2 ~ 11.5		
Ji *et al*. (2011)	1:8	7.5	0.6	0.9	-	Methanol	0.9 ~ 12.6	-	- Smoke on ceilings in a subway station - Max smoke temperature
Ji *et al*. (2012)	1:6	6	0.88	1.76	-	Methanol	3.38 ~ 29.57	-	- Different transverse fire, and max. Temp.
Kashef *et al*. (2013)	1:15	15	0.32	0.224	-	Propane	5.74 ~ 11.48	-	- Ceiling Temp. - Smoke diffusion with natural ventilation
		17					3.2 ~ 14.5		
Hu *et al*. (2013)	-	6	0.8	1.04	0, 3, 5	LPG	20 ~120	0, 0.3, 0.6, 0.9, 1.2	Slope effect
Fan *et al*. (2013)	1:6	6	2	1.76	-	Methanol	3.38 ~ 29.57	Natural ventilation	Transverse smoke Temp.
Lee *et al*. (2012)	-	7	0.6	0.36	-	Gasoline	4.05 ~ 5.81	-	Obstacle effect on ventilation, and critical velocity
			0.4	0.24			4.25 ~ 8.26		
			0.6	0.36			8.54 ~ 10.75		
			0.4	0.24			9.5 ~ 16.01		
Ura *et al*. (2014)	1:12	18	0.5	0.54	-	Heptane	30 ~ 130	Natural ventilation	Roof opening, buoyancy, smoke thickness
Oka *et al*. (2014a)	-	-	2.5	7.25	0-10	Heptane	9.5 ~ 47.4	-	- Ceiling jet in case of inclined tunnels - Temp., and velocity distribution
			10.5	9.8			20 ~ 146.6		
Tanaka *et al*. (2015)	1:5	42	1	2	-	Heptane	85 ~ 253	0.79 ~ 0.95	- Hybrid ventilation strategy
Tang *et al*. (2016)	1:6	72	1.3	1.95	-	LPG	30 ~ 50	0 ~ 1.2	- Effect of ceiling extraction
Fan *et al*. (2016)	1:20	10	0.25	0.075-0.15	-	Heptane, Wood, Plastic	155 ~ 215 63 ~ 106.8 145 ~ 172	-	- Ventilation velocity on ceiling gas Temp., - Heat Flux, and geometry effect
			0.4	0.12, 0.18, 0.24					
Chen *et al*. (2017)	1:9	8	0.8	0.48	-	Methanol	-	-	Sealing ratio, Geometry effect
Zhao *et al*. (2018)	1:15	13	0.48	0.1536	-	Porous gas burner	0, 0.17, 0.22, 0.3, 0.35, 0.4	2.92, 4.31, 5.79, 7.07, 8.45	Fire-induced Temp. in a longitudinal ventilation metro tunnel
Tanaka *et al*. (2018)	1:20	10	0.25	1	-	Propane	0.73 ~ 0.74	0.24 ~ 0.4	- Thermal properties of wall materials - Critical velocity and Back-layering
							1.32 ~ 1.38	0.28 ~ 0.58	
							2.98 ~ 3	0.39 ~ 0.59	
							7.1 ~ 7.17	0.52 ~ 0.71	
							11.91 ~ 11.97	0.55 ~ 0.81	

Tang *et al*. (2019)	1:20	8	0.44	0.1496	-	-	3.7, 4.54, 5.38	0, 0.5, 0.75, 1, 1.5, 2, 2.5	Ceiling extraction velocity, HRR
Lin *et al*. (2019)	1:20	20.8	0.23	0.1035	0 ~ 5	Methanol	2.8, 5.6, 11.2, 16.8	-	Slopes on the self-extinction
Peng *et al*. (2019)	1:20	20.8	0.23	0.1035	0, 1, 5	Methanol	2.8, 5.6, 11.2, 16.8	0, 0.1, 0.3	Slope effect, Self-extinguishing
Huang *et al*. (2019a)	1:15	29.46, 9.23	0.355	0.1331, 0.1686, 0.2396	-	Gas burner	1.72, 2.59, 3.45, 4.31, 5.18, 6.04	0,0.25 ~ 0.91	Bifurcation effect
Zhang *et al*. (2019)	1:15	-	0.075	-	-	Methanol	1 ~ 23	0.258, 0.387, 0.516	Longitudinal ventilation and lateral smoke extraction
Tang *et al*. (2020)	1:8	8	1	2	-	Propane	20.2 ~ 50.4	-	Wall-attached fire with various burner aspect ratios
Wang *et al*. (2020)	1:10	8	0.6	0.3	-	Propane	1.25 ~ 6.25	-	Double fires with different distance
Yao *et al*. (2019a)	1:40	-	-	-	-	Propane, Heptane	0.4 ~ 3.2	-	Self-extinction, and geometry effect
Liu *et al*. (2020)	-	20	1.5	-	-	Diesel	8.94, 26.84, 59.64	-	Geometry effect
Chen *et al*. (2020)	1:10	10	0.6	0.6	-	Propane	15.9 ~ 95.7	0, 0.2, 0.4, 0.6, 0.8, 1	- Bifurcation structure effect - Branch and a longitudinal ventilation
Chaabat *et al*. (2020)	1:25	8.4	0.36	0.0648	-	Air with Helium	0.11 ~ 0.71	-	- Transverse ventilation, exhaust vents effect - Rectangular damper effect

Table 5. A list of scaling correlations for the model tunnel (Ingason and Zhen, 2010; Quintiere, 1989), where subscripts "F" and "M" represent full-scale and model-scale, respectively.

Parameters	Scaling correlation
HRR [kW]	$\dot{Q}_F = \dot{Q}_M (L_F/L_M)^{5/2}$
Mass loss rate [kg/s]	$\dot{m}_F = \dot{m}_M (L_F/L_M)^{5/2}$
Velocity [m/s]	$v_F = v_M (L_F/L_M)^{1/2}$
Time [s]	$t_F = t_M (L_F/L_M)^{1/2}$
Temperature [K]	$T_F = T_M$
Heat flux [kW/m^2]	$\dot{q}''_F = \dot{q}''_M (L_F/L_M)^{1/2}$

For the design of model-scale tests, the key issue is the calculation of similarity to guarantee that the results from the scaled model present those of real-scale tests. The most groundbreaking study in this aspect was the propose of "scaling law" (Quintiere, 2020, 1989). Table 5 lists the classical scaling-law relationships of key fire parameters, including HRR, velocity, and temperature between model- and real-scale fire tests. These formulas incorporate the influences of both material properties and gas flow conditions, based on the controlling non-dimensional numbers of Froude (*Fr*), Reynolds (*Re*), and Richardson (*Ri*) numbers.

The Froude similarity law is used when the number of Reynolds is quite large, the turbulence condition is prevailing, and the buoyancy is dominant. Similar to the compartment fire, *Fr* number has been most widely used in the buoyancy-controlled fire cases, although the turbulence intensity and thermal radiation cannot be explicitly scaled. By the combination with the density ratio of smoke, the effect of stratification can be correlated with a *Ri* number or modified *Fr* number. This approach has been adopted by many researchers (Ingason, 2008; Ingason and Zhen, 2010) and used to study fan performance, backdraft, back-layering, critical velocity, plug-holing phenomenon, etc. More details are discussed in Section 3.

3. Database for existing tunnel-fire research

Fig. 6 shows the key parameters that used to describe the tunnel shape, geometry, ventilation condition, as well as the characteristics of fire and smoke. In this section, the data of seven most widely studied tunnel-fire parameters in the literature, namely, the HRR, flame length, maximum ceiling temperature, smoke layer thickness, critical ventilation velocity for smoke, and the smoke back-layering length, and plug-holing will be summarized to form a database.

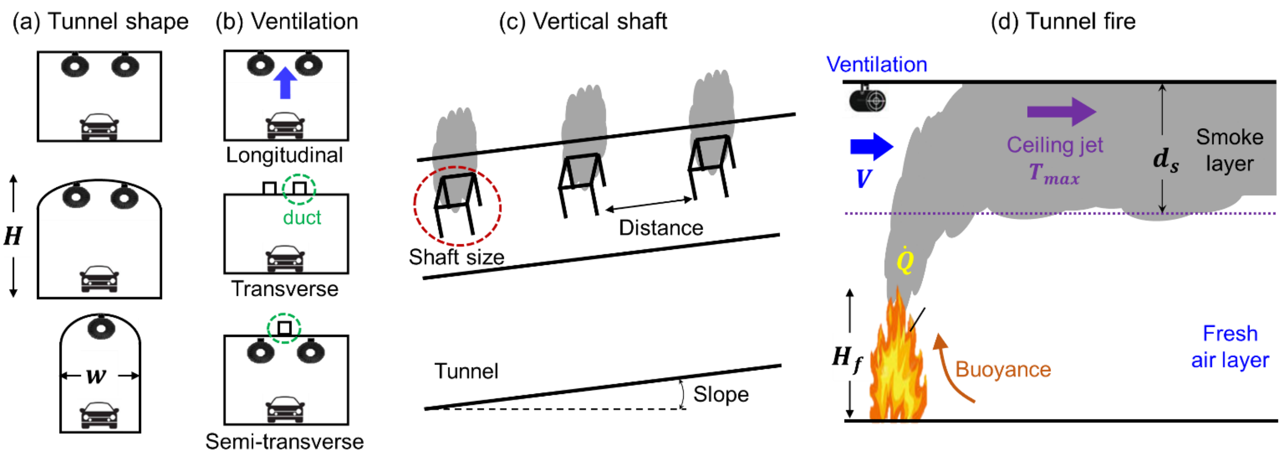

Fig. 6. Diagram for key parameters in tunnel fire research, (a) tunnel shape, (b) ventilation, (c) verticl shaft, and (d) tunnel fire and smoke.

3.1. Fire heat release rate in tunnel

Heat release rate (HRR) is one of the most important parameters in fire to describe the size and severity of the fire, which is also applied to the tunnel fire. The value of HRR is also closely related to other parameters, such as flame length and critical ventilation velocity. Because the primary fuel load in the tunnel is the vehicle and goods, for these real-scale tests, the fire source often uses real burning vehicles or simulated by liquid pool fires or gas burners, based on the measurements of the vehicle fire. The peak heat release rate (pHRR) of vehicle depends on the type of vehicle (small, large, electrical vehicles, etc.) and ventilation conditions, which requires the burning of full-scale vehicles (see Fig. 2).

Table 6 summaries the value of pHRR of burning different types and numbers of vehicles in open and confined spaces (e.g. parking lots, underground spaces, and tunnels). In general, the pHRR is 1-5 MW for small passage cars (Ingason, 2001; Okamoto et al., 2009; Sun et al., 2020), 1-10 MW for large passage cars (Edith, 1996; Mohd Tohir and Spearpoint, 2013; Okamoto et al., 2009), 10-50 MW for buses and HGVs (Bettelini et al., 2016; Hammarström et al., 2008; Steinert, 1994), and 300-430 MW for oil tankers (Larson *et al.*, 1983).

Table 6. The pHRR from burning different types and numbers of vehicles in open and confined spaces, where * means not conducted in tunnel, engine displacements of small and large passenger cars are 1,500 cc and 3,000 cc, respectively.

References	Types of vehicle	HRR [MW]	Conditions
Okamoto *et al*. (2009) *	small passenger car	3.5	Four full-scale fire experiments using small passenger cars for varying location of fires
	large passenger car	4.2	
Shipp *et al*. (1995) *	small passenger car	8	Using calorimeter hoods for investigating full-scale vehicle fires
Ingason (2001)	small passenger car	2.5	HRR are densely caused by many other factors, such as ventilation performance, ceiling temperatures, as the fire test was performed in a real tunnel (Park *et al*., 2019).
	large passenger car	<5	
	2 passenger cars	3.5-10	
Park *et al*. (2019) *	small passenger car	3.5	Using a large-scale cone calorimeter, which can be applicable up to 20 MW, and 1500cc real vehicles in large space, not in a tunnel
	2 passenger cars	6	
Mangs *et al*. (1994) *	small passenger car	1.5-2	Using an oxygen calorimetry hood with heptane
Edith (1996) *	small passenger car	4.1	Using different types and numbers of passenger car inside closed parking lot.
	large passenger car	8.3	
	2 small passenger cars	7.5	
	2 large passenger cars	8.3	
Steinert (1994)	various types of passenger cars	1.7-4.6	Experiments in a parking lot with the front window open
	2 or 3 passenger cars	5.6-8.9	
	Bus with 40 seats	34	EUREKA 499 project
Ingason *et al*. (2015a)	2 small passenger cars	3	Ventilation effect on HRR
		4.6	Fixed ventilation performance of 6 m/s
Mohd *et al*. (2013) *	small passenger car	1.8-4	Various experiments for the initial ignition location and various size of vehicles
	large passenger car	1.5-8.8	
	SUV	0.5-1.5	
Hammarström *et al*. (2008) *	Bus with 49 seats	25	Using a large good calorimeter which can be applicable 10 MW and gas burner for ignition.
Haack (1998) (EUREKA 499 test)	Mock-up HGV/HGV	23/128	
Bettelini *et al*. (2016) (Mont Blanc test)	HGV	23	trailer contains 400 kg margarine
Ingason *et al*. (2015a) (2nd Benelux test)	HGV	13,19,16	Focusing on ventilation performances with a range of 0.5m/s to 5 m/s
Ingason *et al*. (2005) (Runehamar test)	mock-up HGV-trailer	66-202	2.8-3.2 m/s of initial longitudinal ventilation rates
Larson *et al*. (1983) (Caldecott test)	tanker fires	300-430	Simulate gasoline tanker accident, assuming 430 MW full-scale fire, but knowledge about the effect of ventilation in the event of such a large fire was still unclear.
Hansen (2015)	mining vehicle	16-30	Mining vehicle test in a tunnel

In the model-scale tunnel fire tests, burning a full-scale vehicle is clearly inappropriate. Instead, researchers often use the well-controlled gas fuel burner and liquid fuel fire to mimic the burning of vehicles. Then, the characteristic HRR and pHRR can be set based on the nondimensional analysis (see Table 5), depending on the real-scale HRR, as well as the shape and scale of the tunnel model. The typical HRR of typical model-scale tunnel fire tests are summarized in Table 4.

3.2. Flame length

The flame length refers to a characteristic size of the flame (Drysdale, 2011). For the tunnel fire, the flame height (H_f) of a non-impinging flame (see Fig. 6d) and the flame (extension) length (L_f) of a impinging flame (Fig. 7) are most widely used and studied. Both are key parameters, because it not only indicates the fire HRR and turbulent behavior but also determines the fire spread rate and fire impact on the structure. Previous studies showed that fire flame length could be correlated with burner size and proposed a widely accepted formula of $L_f/D{\sim}1.7$ (Blinov and Khudiakov, 1961). Thomas *et al.* (1961) did several wood crib experiments taking into account the density of fuel and volume flow. Steward (1970) established a theory based on conservation equations, which was further simplified by Fang (1973). McCaffrey (1979) proposed to calculate the flame length by separating the whole flame into a continuous flame region and an intermittent flame region. Table 7 summaries the empirical correlations for flame height (H_f) if it does not reach the ceiling.

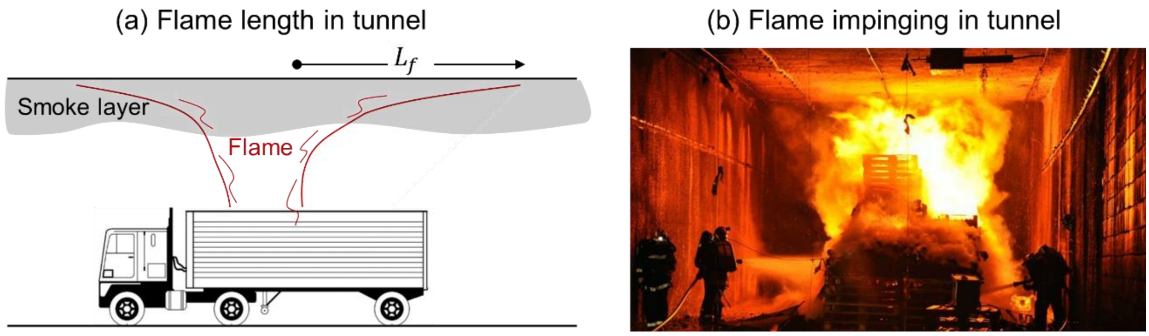

Fig. 7. (a) Diagram of flame (extension) length when flame impinges the tunnel ceiling, and (b) photo of the flame impinging in a tunnle.

Table 7. Derived formulas for investigating on flame height in an open space.

Authors/Projects	Proposed equation	Conditions
Blinov (1957)	$\frac{H_f}{D} \propto 1.7$	Flames above circular pans of burning liquids
Thomas *et al*. (1961)	$\frac{H_f}{D} \propto \left[\frac{\rho v^2}{D^5}\right]^n$	Considered the cold fuel density and volume flow rate, and exponent n is around 0.3
Thomas (1963)	$H_f = 18\dot{m}^{2/5}$	$\dot{m}$ fuel flow rate
Fang (1973)	$\frac{H_f}{D} \propto \frac{K}{2^{4/5}} = Fr^{1/5}$ $H_f = 0.37K\dot{m}^{2/5}$	$Fr = \frac{(\dot{m}/A)^2}{\rho_a^2 gD}$ A0 is the source area rrD2/4 26 < K < 60 based on the data
McCaffrey (1979)	$H_f = C\dot{Q}^{2/5}$	C = 0.08, in continuous flame region C = 0.20, in intermittent flame region
Heskestad (2016)	$H_f = 0.23\dot{Q}^{2/5} - 1.02D$	Suitable for turbulent diffusion flames

For the flame extension length (L_f), Rew *et al.* (1999) proposed a method of considering the ceiling jet in unconfined ceilings, while this method cannot be applied to scenarios where flame length is substantially large. Recent studies on the flame length of a tunnel fire are mainly focus on flame extension length (i.e., the length of ceiling jet flame), and numerous equations are proposed to estimate the flame extension length, e.g. (Gao et al., 2017; Ji et al., 2015a; Lattimer et al., 2013; Wan et al., 2017). Typically, the flame extension length can be expressed in the nondimensional form with a characteristic length (L), such as the diameter of the flame (D) and the height of tunnel (H), as

$$\frac{L_f}{L} = \alpha\left(\dot{Q}^*\right)^n \quad (1)$$

where α and n are fitting coefficient. Table 8 summaries the empirical correlations for the flame extension length (L_f) in the confined space that are used often in tunnel fire.

Table 8. Derived formulas for investigating on flame height in a confined space.

Authors/Projects	**Proposed equation**	**Conditions**
You *et al.* (1979)	$\frac{L_f}{D} = 0.502\left(\frac{H_{fr} - H_{ef}}{D}\right)^{0.957}$	H_{fr} is free flame height
Hasemi *et al.* (1997)	$\frac{L_f}{D} = 2.58\dot{Q}^{*\frac{2}{5}}(H/D)^{2/5} - H/D$	$\dot{Q}^* = \frac{\dot{Q}}{\rho_a C_p T_a g^{1/2} D^{5/2}}$
Rew *et al.* (1999)	$L_f = 0.02\left(\frac{\dot{Q}}{120}\right)\left(\frac{V}{10}\right)^{-0.4}$	Cannot apply in real tunnels as the size of the tunnel did not into account.
Lönnermark *et al.* (2006)	$L_f = \frac{1370\dot{Q}^{0.8}V^{-0.4}}{(T_f - T_a)^{3/2} H^{3/2}}$	Considered air velocity Primarily used in the ceiling jets in unconfined ceilings, which has limitation to apply for all situations.
Ingason *et al.* (2010)	$\frac{L_f}{H} = 4.3\dot{Q}^*$	$\dot{Q}^* = \frac{\dot{Q}}{\rho_a C_p T_a \sqrt{g H_{ef}} A}$
Ding *et al.* (2012)	$\frac{L_f}{D} = 1.62\dot{Q}^{*\frac{2}{5}}$	$\dot{Q}^* = \frac{\dot{Q}}{\rho_a C_p T_a g^{1/2} D^{5/2}}$
Lattimer (2013)	$\frac{L_f}{H_{ef}} = 3.1\dot{Q}^{*\frac{2}{5}} - 1$	$\dot{Q}^* = \frac{\dot{Q}}{\rho_a C_p T_a g^{1/2} H^{5/2}}$
Zhang *et al.* (2014)	$\frac{L_f}{D} = 24.49\left[\frac{(H_{fr} - H_{ef})u}{H_{fr}\sqrt{g H_{ef}}}\right]$	For cylindrical flame shape hypothesis H_{fr} is free flame height
Gao *et al.* (2015)	$\frac{L_f + H_{ef}}{H_{ef}} = \begin{cases} 2.0\dot{Q}^{*\frac{1}{2}}, \text{longitudinal} \\ 3.0\dot{Q}^{*\frac{2}{5}}, \text{transverse} \end{cases}$	For fire flush with sidewall $L_f + H_{ef}$ is total flame extension length
	$\frac{L_f + H_{ef}}{H} = 1.6\dot{Q}^{*\frac{2}{5}}$	For fire at the longitudinal centerline is symmetrical
	$\frac{L_f}{D} = 3.0\dot{Q}^{*\frac{2}{5}}$	in the open $\dot{Q}^* = \frac{\dot{Q}}{\rho_a C_p T_a g^{1/2} D^{5/2}}$
	$\frac{L_f}{D} = 3.2\dot{Q}^{*\frac{1}{2}}$	wall fire without ceiling
Ji *et al.* (2015a)	$\frac{L_f + H_{ef}}{H_{ef}} = 1.02\dot{Q}_{BH_{ef}}^{*1.25} + 1$	Longitudinal length of ceiling jet flame $\dot{Q}_{BH_{ef}}^* = \frac{\dot{Q}}{\rho_a C_p T_a g^{1/2} B H_{ef}^{3/2}}$ B is pan edge perpendicular to the sidewall
Wan *et al.* (2017)	$\frac{L_{ef}}{6D + 2S} = \begin{cases} 4.29\dot{Q}_G^{*0.46}, \text{open space} \\ 2.50\dot{Q}_G^{*0.42}, \text{for tunnel} \end{cases}$	For two flames, S is burner spacing (m) $\dot{Q}_G^* = \frac{2\dot{Q}^*}{(6+2S/D)^{5/2}}$ for group flames
Zhang *et al.* (2017)	$\frac{L_f}{H} = 2.84\dot{Q}_{Hm}^{**0.53}$	$\dot{Q}_{Hm}^{**}$ is non-dimensional HRR, which related to volume of a free flame, angle and other shape factors.
Gao *et al.* (2017)	$\frac{L_{f\,max}}{D} = 3.3\dot{Q}_{ef}^{*1/4}$ (Maximum length) $\frac{L_{f\,avg}}{D} = 2.3\dot{Q}_{ef}^{*1/4}$ (Average length)	$\dot{Q}_{ef}^* = \frac{\dot{Q}_{ef}}{\rho_a C_p T_a g^{1/2} D^{5/2}}$
Qiu *et al.* (2018)	$\frac{L_{f\,t}}{D} = 104.02\left(\frac{H_{fr} - H/\cos\theta}{H_{fr}}\right)\dot{Q}_{fuel}^{**}$ $0.199 \le \dot{Q}_F^* \le 0.427$, $0.3 \le V \le 1.8$	$L_{f\,t}$ total extension lengths of up and down stream θ flame tilt angle (degree); H_{fr} free flame height $\dot{Q}_F^* = \frac{\dot{Q}_{fule}}{\rho_a \Delta H_a (gH)^{1/2} wD}$, ΔH_a heat released per kg of air consumed (kJ/kg)

3.3. Maximum ceiling gas temperature

The maximum ceiling gas temperature is a significant parameter in tunnel fire research, and a lot of related studies have been done in last serval decades. Alpert (1975) firstly investigated the maximum smoke temperature beneath ceiling and proposed equations to estimate the maximum ceiling gas temperature in an unconfined ceiling. Then, Kurioka *et al.* (2003) conducted tests on both the model scale and real scale, considering the parameters of the tunnel cross-section area, HRR, and mechanical ventilation speed. The flame tilt, flame height, maximum gas temperature, and the flame location were measured. An empirical correlation in the form of exponential function considering those parameters was then proposed (Kurioka *et al*., 2003), and excellent predictions were obtained (Meng *et al*., 2017; Tang *et al*., 2019). Li *et al.* (2011; 2012) conducted model-scaled tunnel fire tests taking into account the influences of HRR, longitudinal ventilation speed, and tunnel geometries. However, the effect of slope, which is regarded as a decisive factor affecting the temperature distribution, was not considered. To address the slope effect, more tests were performed in tunnels with a scale factor of 1:20 (Hu *et al*., 2013). Until recently, studies showed that many factors, such as bifurcation of structure, portal sealing and blockage also have remarkable effect on maximum temperature under the forced ventilation condition (Huang *et al*., 2019a, 2019b, 2018).

The correlation between the maximum temperature and other parameters has been explored by many researchers. They proposed many empirical formulas or models to calculate the maximum gas temperature rise beneath the ceiling in recent years, e.g. (Hu et al., 2013; Ji et al., 2011; Li et al., 2011; Fei Tang et al., 2017b; Tang et al., 2018a), most of their models can be expressed as

$$\Delta T_{max} = \alpha \frac{\dot{Q}^{2/3}}{H_{ef}^{5/3}} \tag{2}$$

where coefficient α usually around 16.9 to 17.9 (Yao *et al*., 2018). Table 9 summarizes the formula proposed to calculate the highest ceiling temperature varying with variables of HRR, tunnel geometry, *Fr*, *Re*, and ventilation performances.

Table 9. Derived formulas for investigating maximum temperature

References	Proposed equation	Conditions
Alpert (1975)	$\Delta T_{max} = T_a + 16.9\frac{\dot{Q}^{2/3}}{H^{5/3}}$	
Heskestad *et al.* (1979)	$\Delta T^* = \begin{cases} 6.3 & \frac{r}{H} \leq 0.2 \\ (0.188 + 0.313r/H)^{-4/3} & 0.2 < r/H < 4.0 \end{cases}$	$\Delta T^* = \frac{\Delta T/T_a}{\dot{Q}^{*2/3}}, \dot{Q}^* = \frac{\dot{Q}}{\rho_a T_a C_p g H^{5/2}}$
Kurioka *et al.* (2003)	$\Delta T_{max} = \gamma T_a \left(\frac{\dot{Q}^{*2/3}}{Fr^{1/3}}\right)^{\varepsilon}$	$\frac{\dot{Q}^{*\frac{2}{3}}}{Fr^{\frac{1}{3}}} < 1.35, r = 1.77, \varepsilon = \frac{6}{5}$ $\frac{\dot{Q}^{*\frac{2}{3}}}{Fr^{\frac{1}{3}}} > 1.35, r = 2.54, \varepsilon = 0$
Li *et al.* (2011;2012)	$\Delta T_{max} = \begin{cases} 17.5\frac{\dot{Q}^{2/3}}{H_{ef}^{5/3}}, V^* \leq 0.19 \\ \frac{\dot{Q}}{V b_f^{\frac{1}{3}} H_{ef}^{\frac{5}{3}}}, V^* > 0.19 \end{cases}$	$V^* = V/(\frac{\dot{Q}_c g}{b_f \rho_a c_p T_a})^{1/3}$ $\Delta T < 1350$ K (in case of horizontal tunnel)
Ji *et al.* (2011)	$\Delta T_{max} = 16.9\frac{\dot{Q}^{2/3}}{H_{ef}^{5/3}}\left(0.299e^{-0.793d/H_{ef}} + 1\right)$	d: distance between fire to end wall
Ji *et al.* (2012)	$\Delta T_{max} = 17.9\frac{\dot{Q}^{2/3}}{H_{ef}^{5/3}}\left(1.096e^{-14.078d/(\frac{W}{2})} + 1\right)$	For different transverse fire locations. d is distance between the fire and the sidewall.

Fan *et al.* (2013)	$\Delta T_{max}=17.9\frac{\dot{Q}^{2/3}}{H_{ef}^{5/3}}\left(1.096e^{-14/(\frac{w}{2})}+1\right)\left(0.893e^{-3.7d_f/w}+0.107\right)$	d is distance between the fire and the sidewall, d_f is the distance away from the fire.
Hu *et al.* (2013)	$\Delta T_{max}=\begin{cases}(1-0.061\beta)17.5\frac{\dot{Q}^{2/3}}{H_{ef}^{5/3}}, V^*\le 0.19\\(1-0.067\beta)\frac{\dot{Q}}{Vb_f^{1/3}H_{ef}^{5/3}}, V^*>0.19\end{cases}$	$V^*=V/\left(\frac{\dot{Q}_c g}{b_f\rho_a c_p T_a}\right)^{1/3}$ (correction for the slope)
Gao *et al.* (2014)	$\Delta T_{max}=\begin{cases}1000\dot{Q}^{*1/2}, 0.22<\frac{d}{H_{ef}}<1.11\\1318\dot{Q}^{*1/2}\text{ (safety door)}\end{cases}$	$\dot{Q}^*=\dot{Q}/\rho_a c_p T_a\sqrt{gH_{ef}^5}$
Ji *et al.* (2015b)	$\frac{\Delta T_{max}}{T_a}=\dot{Q}^{*0.56}(2.37+0.89e^{16.10\beta})e^{(-0.05-166.38\beta^{2.31})(\frac{r}{H})}$	r is distance from the fire source to the measuring point.
Meng *et al.* (2017)	$\Delta T_{max}=\begin{cases}1.256T_a\dot{Q}^{*3.65}\text{ (screen door)}\\1.256T_a\dot{Q}^{*2.92}\text{ (safety door)}\end{cases}$	$\dot{Q}^*=\dot{Q}/\rho_a c_p T_a\sqrt{gH_{ef}^5}$
Tang *et al.*(2017)	$\Delta T_{max}=\begin{cases}\dot{Q}/V\left(\frac{D}{2}\right)^{\frac{1}{3}}H_{ef}^{\frac{5}{3}}, & V^*>0.19, v=0\\\frac{(0.49v^*+0.73)\dot{Q}}{V\left(\frac{D}{2}\right)^{\frac{1}{3}}H_{ef}^{\frac{5}{3}}}, & V^*>0.19, 0.5\le v\le 2.2\\17.5\,\dot{Q}/H_{ef}^{\frac{5}{3}}, & V^*\le 0.19, v=0\\\frac{(0.49v^*+0.73)\dot{Q}}{V\left(\frac{D}{2}\right)^{\frac{1}{3}}H_{ef}^{\frac{5}{3}}}, & V^*\le 0.19, 0.5\le v\le 2.2\end{cases}$	v is ceiling extraction velocity (m/s). v^* is dimensionless ceiling extraction velocity. $v^*=\frac{v}{\sqrt{gH_{ef}}}$ $V^*=V/\left(\frac{\dot{Q}_c g}{b_f\rho_a c_p T_a}\right)^{1/3}$
Zhou *et al.* (2017a)	$\Delta T_{max}=17.5\frac{\dot{Q}^{2/3}}{H_{ef}^{5/3}}\left(2.19e^{-16.42d/(\frac{w}{2})}+0.97\right), V^*\le 0.19$	For different transverse fire locations. d is distance between the fire and the sidewall.
Tang *et al.* (2018a)	$\Delta T_{max}=\left(-30.7\frac{vA_{sh}}{\sqrt{gH_{ef}}}+1\right)\{9.35e^{[-0.45(n-1)]}11.49\}*\frac{\dot{Q}^{2/3}}{H_{ef}^{5/3}}$	Rectangular-source fires, with two-point extraction. v is ceiling extraction velocity (m/s). n is burner aspect ratio.
Huang *et al.* (2018)	$\Delta T_{max}=\begin{cases}\left(0.965+0.352\left(\frac{h}{H}\right)\right)17.5\frac{\dot{Q}^{2/3}}{H_{ef}^{5/3}}, \dot{Q}\le 50MW\\\left(0.946-0.097\left(\frac{h}{H}\right)\right)17.5\frac{\dot{Q}^{2/3}}{H_{ef}^{5/3}}, \quad \dot{Q}>50MW\end{cases}$	h is sealing height. $\frac{h}{H}$ is sealing ratio. $V^*\le 0.19$,
Huang *et al.* (2019a)	$\Delta T_{max}=\begin{cases}2.5\left(\frac{\dot{Q}}{T_a c_p\rho_a\sqrt{g(0.95H_{ef}-z_0)^5}}\right)^{2.5}, V^*\le 0.19\\a\left(1.71V'^{-\frac{5}{6}}\left(\frac{\dot{Q}}{T_a c_p\rho_a\sqrt{gH_{ef}^5}}\right)^{\frac{2}{3}}\right)^b, V^*>0.19\end{cases}$	$V^*=V/\left(\frac{\dot{Q}_c g}{b_f\rho_a c_p T_a}\right)^{1/3}$ $\begin{cases}a=1.332-3.548\sin\alpha+9.889\sin^2\alpha\\b=0.979-4.464\sin\alpha+13.833\sin^2\alpha\end{cases}$ α: dimensionless expression z_0: virtual origin height (m)
Huang *et al.* (2019b)	$\Delta T_{max}=\left(15.336-3.398\frac{l}{H_{ef}}\left(\frac{V}{\sqrt{gH_{ef}}}\right)^{1/3}\right)\frac{\dot{Q}^{2/3}}{H_{ef}^{5/3}}$	l is distance between fire source and blockage (m).
Tang *et al.* (2019)	With ceiling smoke extraction: $\Delta T_{max}=\begin{cases}(0.71v^*+1)33.55\,\dot{Q}^{2/3}/H_{ef}^{5/3}, v^*\le 0.55\\(-0.33v^*+1.57)33.55\,\dot{Q}^{2/3}/H_{ef}^{5/3}, v^*>0.55\end{cases}$ $\Delta T_{max}=33.55\,\dot{Q}^{2/3}/H_{ef}^{5/3}$ (no ceiling smoke extraction)	v is ceiling extraction velocity(m/s). $v^*$is dimensionless ceiling extraction velocity. $v^*=v/\sqrt{gH}$

3.4. Critical ventilation velocity of back-layering

The smoke ventilation capability remains the central issue for tunnel fire safety. The critical velocity of smoke ventilation (V_c) is defined as the minimum longitudinal ventilation velocity that prevents the upstream movement of the combustion product from fire. In cases where the ventilation speed is too weak to prevent the smoke flows backward, the so-called back-layering phenomenon occurs. Fig. 8 shows a schematic diagram of smoke ventilation and back-layering phenomenon. Since the fire smoke or emission gases are usually toxic, the main research goal in this area is to optimize the design of tunnel ventilation systems for safe evacuation.

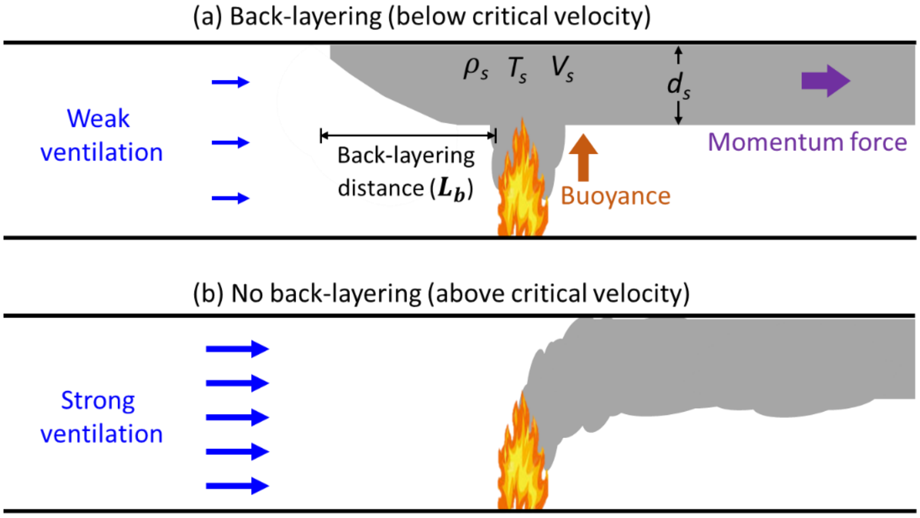

Fig. 8. Schematic diagrams of the critical velocity for smoke back-layering; (a) back-layering occurs under weak ventilation, and (b) smoke stays in one side of the fire under strong ventilation.

Thomas (1968) defined a term of the critical Froude number (Fr_c) as the ratio of the buoyancy force of smoke flow to the inertial force of ventilation airflow. Based on the definition, he first developed the critical Froude theory and suggested that ideally the smoke backflow disappears when the critical Froude number equals to 1. However, later results of a reduced-scale tunnel (Calvin K Lee *et al.*, 1979) showed that the critical Froude number ranged from 4.5 to 6.7, if the dimensionless HRR (Q^*) was larger than 1.3 (Kennedy and Parsons, 1996). Therefore, a constant critical Froude number may not be suitable for all tunnel fire scenarios. Oka *et al.* (1995) conducted a small-scale experiment to obtain the relationship between critical velocity and HRR considering the effect of burner size, based on which a new dimensionless equation was then proposed. Subsequently, Wu *et al.* (2000) conducted another five tests with fixed tunnel height while varying hydraulic diameter. However, it should be kept in mind that in these tests (Oka and Atkinson, 1995; Wu and Bakar, 2000), water spray devices were used to protect the model tunnel, which may enhance the heat loss of smoke flow and decrease the buoyancy force head, and hence cause a lower test value of critical velocity. Other parameters influencing the critical velocity of tunnel geometry (Li *et al.*, 2010; Wu and Bakar, 2000), blockage (Zinoubi and Ben, 2019) fire size (Oka and Atkinson, 1995), and tunnel slope (Kennedy and Parsons, 1996) were also investigated.

The aspect ratio of tunnel width over tunnel height is another important factor influencing critical velocity, and some studies also adopted hydraulic diameter as the characteristic length. In fact, tunnel height and width mainly influenced the vertical plume and transverse smoke, respectively. However, they are equivalent in the calculation of hydraulic diameter. The term of hydraulic diameter cannot reflect the influencing mechanism of tunnel shape. To tackle this problem, Kunsch (2002) proposed a theoretical model that was based on Alpert's work on ceiling jets (Alpert, 1975) but also included the aspect ratio. Li *et al.* (2010; 2017) proposed a model based on a set of model-scaled tests and corresponding numerical simulation. Weng *et al*. (2015) also proposed a model to predict critical velocity with model scale tests and CFD simulations. Table 10 lists test details on studying V_{cr}, and Table 11 summarizes the derived empirical correlations.

Table 10. General information and data of tunnel fire tests to investigate the critical velocity.

Parameters	Length [m]	Width [m]	Height [m]	Aspect Ratio	Slope [º]	Fuel/Fire [kW]	Ventilation [m/s]	V_c [m/s]
Longitudinal ventilation (Oka and Atkinson, 1995)	15	0.274	0.244	1.12	-	Propane 1-78	0.12-0.52	0.16-0.27
Slope effect (Atkinson and Wu, 1997)	15	0.274	0.244	1.12	0-10	Propane, 5	0.4-2	0.67-0.75
						13.5		0.65-0.71
						26.9		0.64-0.69
Geometry of cross-section (Wu and Bakar, 2000)	15	0.136	0.25	0.544	-	Propane 1.5-30	-	0.43-0.48
		0.25		1				0.39-0.6
		0.5		2				0.37-0.65
		1		4				0.34-0.65
Channel dimension (Vauquelin, 2005)	-	0.5	0.25	2	0-10	0.1-10	-	0.35-0.51
Geometry of aspect ratio (Lee and Ryou, 2005)	10.4	0.6	0.3	0.5	-	Ethanol 2.47-12.3	-	0.4-0.54
		0.5	0.333	0.667				0.42-0.55
		0.4	0.4	1				0.45-0.59
		0.333	0.5	1.5				0.45-0.61
		0.3	0.4	2				0.47-0.64
Geometry of tunnel width (Vauquelin and Wu, 2006)	18	0.136	0.25	0.544	-	Propane 1.4-28	-	0.34-0.43
		0.25	0.25	1				0.4-0.46
		0.5	0.25	2				0.475-0.56
		1	0.25	4				0.478-0.6
Longitudinal ventilation (Roh *et al*., 2008)	10	0.4	0.4	1	-	Heptane, 2.23-15.6	0-1.68	2.82-4.12
Correlation between back-layering (Li *et al*., 2010)	12	0.25	0.25	1	-	Propane 0.7-16.7	-	0.33-0.67
		0.45	0.393	0.11		2-18.4		0.43-0.82
Critical velocity near exits (Tsai *et al*., 2011)	4	0.6	0.6	1	-	Gasoline 0-9	-	0.28-0.62
Obstacle effect (Lee and Tsai, 2012)	7	0.6	0.6	1	-	Gasoline 4.05-8.26	0-10	0.32-0.62
		0.4	0.4			8.54-16.01		0.43-0.85
Slope effect (Chow *et al*., 2015)	8	1.5	1	1.5	0	Gasoline 32.6-48.1	1-1.5	1.7-1.9
					2			2-2.2
					4			2.2-2.6
					5			2.5-2.8
					6			2.8-3.2
Ceiling exhaust vent (Tang *et al*., 2018b)	8	0.34	0.44	0.77	-	Propane, 1.5-18	0-2.7 (ceiling)	0.25-8.1

Table 11. Derived formulas for investigating critical velocity

References	**Critical velocity**	**Conditions and comments**
Thomas (1968)	$V_c = k(\frac{g\dot{Q}'_a}{\rho_a C_p T_g})^{1/3}$	Considered the effect of ventilation velocity and the HRR k is a constant and was determined from suitable experiments
Hinkley (1970)	$V_c = K'(\frac{g\dot{Q}_c T_g}{\rho_a C_p T_a^2 w})^{1/3}$	$K' = 0.8$ is determined from experimental data of hot gas layers in short corridors without ventilation velocity.
Heselden (1976)	$V_c = CK(\frac{g\dot{Q}_c T_g}{\rho_a C_p T_a^2 w})^{1/3}$	$K = 0.8$
Danziger *et al.* (1982)	$V_c = 0.606(\frac{g\dot{Q}_c H}{\rho_a C_p T_g A})^{1/3}$	This model is based on the researches by Lee *et al.* (C. K Lee *et al.*, 1979) and Feizlmayr (Feizlmayr, 1976), in which when Fr is less than 4.5, where the smoke back-layering can be stopped
Oka *et al.* (1995)	$V^* = K_v\left(\frac{\dot{Q}^*}{0.12}\right)^{1/3} \quad (\dot{Q}^* \le 0.12)$ $V^* = K_v \quad \dot{Q}^* > 0.12)$	$0.22 < K_v < 0.38,\ \dot{Q}^* = \frac{\dot{Q}}{\rho_a C_p T_a g^{\frac{1}{2}} H^{\frac{5}{2}}},\ V^* = \frac{V}{\sqrt{gH}}$ K_v is varied according to the types of fuel
Kennedy *et al.* (1996)	$V_c = K_g k(\frac{g\dot{Q}_c H}{\rho_a C_p T_g w})^{1/3}$	K_g is a grade correction factor for slope, and k = 0.61 is calculated based on a modified Froude number equal to 4.5
Wu *et al.* (2000)	$V^* = 0.4[0.2]^{-\frac{1}{3}}[\dot{Q}^*]^{\frac{1}{3}} \quad (\dot{Q}^* \le 0.2)$ $V^* = 0.4, \quad (\dot{Q}^* > 0.2)$	$Q^* = \frac{\dot{Q}}{\rho_a C_p T_a g^{1/2} H^{5/2}},\ V^* = \frac{V}{\sqrt{gH}}$ Considered critical velocity and the hydraulic diameter of the tunnel (Li *et al.*, 2010).
Kunsch (2002)	$V^* = 1.52(\dot{Q}^*)^{1/3}\frac{\sqrt{C_1 + (C_1 - C_2)6.13\dot{Q}^{*2/3}}}{1 + 6.13(\dot{Q}^*)^{2/3}}$	$C_1 = \frac{1-\frac{0.1H}{w}}{1+\frac{0.1H}{w}}\left[1 + \frac{0.1H}{w} - 0.015\left(\frac{H}{w}\right)^2\right]$ $C_2 = 0.574\left[\frac{1 - 0.1H/w}{1 + 0.1H/w}\right][1 - 0.2(H/w)]$ - Theoretical analysis of smoke movement in a tunnel without the effect of ventilation based on Alpert's theory (Alpert, 1975) of ceiling jets under unconfined ceilings.
Lee *et al.* (2005)	$V_c = 0.73A_s^{0.2}\sqrt{gH}(\frac{\dot{Q}}{\rho_a C_p T_a\sqrt{A_s g H^5}})^{1/3}$	Considered the effect of aspect ratio of tunnel and vertical shaft, and A_s is aspect ratio.
Hu *et al.* (2008)	$V_c = \left[C_K gH\gamma\dot{Q}^{*\frac{2\varepsilon}{3}}(gH_{ef})^{\frac{\varepsilon}{3}}\right]^{1/(2+2\varepsilon)}$	$Fr = V^2/gH_{ef}, C_K$ =0.2-0.4 $\dot{Q}^{*\frac{2}{3}}/Fr^{\frac{1}{3}} < 1.35, \gamma = 1.77, \varepsilon = \frac{6}{5},$ $\dot{Q}^{*\frac{2}{3}}/Fr^{\frac{1}{3}} > 1.35, \gamma = 2.54, \varepsilon = 0$
Li *et al.* (2010)	$V^* = \begin{cases} 0.81Q^{*1/3}, \dot{Q}^* \le 0.15 \\ 0.43, \quad \dot{Q}^* > 0.15 \end{cases}$	$\dot{Q}^* = \frac{\dot{Q}}{\rho_a C_p T_a g^{1/2} H^{5/2}},\ V^* = \frac{V}{\sqrt{gH}}$
Yi *et al.* (2014)	$V_c = (1 - 0.034\beta)V_{c,0}$	$V_{c,0}$ is critical velocity of the corresponding horizontal tunnel. β is tunnel slope in % (correction for the slope).
Weng *et al.* (2015)	$V^* = 0.82\dot{Q}^{*1/3}$	$Q^* = \frac{\dot{Q}}{\rho_a C_p T_a g^{1/2}\bar{H}^{5/2}},\ V^* = \frac{V}{\sqrt{g\bar{H}}}$
Li *et al.* (2017)	$V^* = \begin{cases} 0.81(A_s)^{-1/12}Q^{*1/3}, \dot{Q}^* \le 0.15A_s^{-\frac{1}{12}} \\ 0.43, \quad \dot{Q}^* > 0.15A_s^{-\frac{1}{12}} \end{cases}$	$\dot{Q}^* = \frac{\dot{Q}}{\rho_a C_p T_a g^{1/2} H^{5/2}},\ V^* = \frac{V}{\sqrt{gH}},\ A_s = w/H$ Aspect ratios of 1 and 1.15 for critical velocity and back-layering length with FDS simulation.
Jiang *et al.* (2018b)	$V_{c-ob} = (1 - 0.545\varphi)V_c$	V_{c-ob} is critical velocity with blockage. φ is blockage ratio (correction for the blockage effect).
Tang *et al.* (2018b)	$V^{*^*} = \begin{cases} 0.81Q^{*^*1/3}, \dot{Q}^* \le 0.13 \\ 0.42, \quad \dot{Q}^* > 0.13 \end{cases}$	Considering the effect of ceiling extraction. $Q^{*^*} = \frac{\dot{Q} - c_p\dot{m}\Delta T_{max}}{\rho_a C_p T_a g^{1/2}\bar{H}^{5/2}},\ V^* = \frac{V}{\sqrt{g\bar{H}}}$

Typically, there are two ways to represent the critical velocity of smoke ventilation, that is, the dimensional and the non-dimensional forms as

$$V_c = K\left(\frac{g\dot{Q}_c}{\rho_a C_p T w}\right)^{1/3}, \quad V^* = K\dot{Q}^{*1/3} \tag{3}$$

The selected empirical correlations are drawn in Fig. 9 for comparison, where both (a) dimensional form (V_c) and (b) non-dimensional form (V^*) are presented in comparison. As the parameters considered in various equations are different, for clear displaying, the aspect ratio and the hydraulic diameter were set as 0.25 and 16, respectively (Lee and Ryou, 2005), and the values of all the other parameters were set based on the work by Wu *et al.* (2000). Basically, most of the empirical correlations following the scaling law in terms of the Froude number can calculate the characteristic values of speed and length.

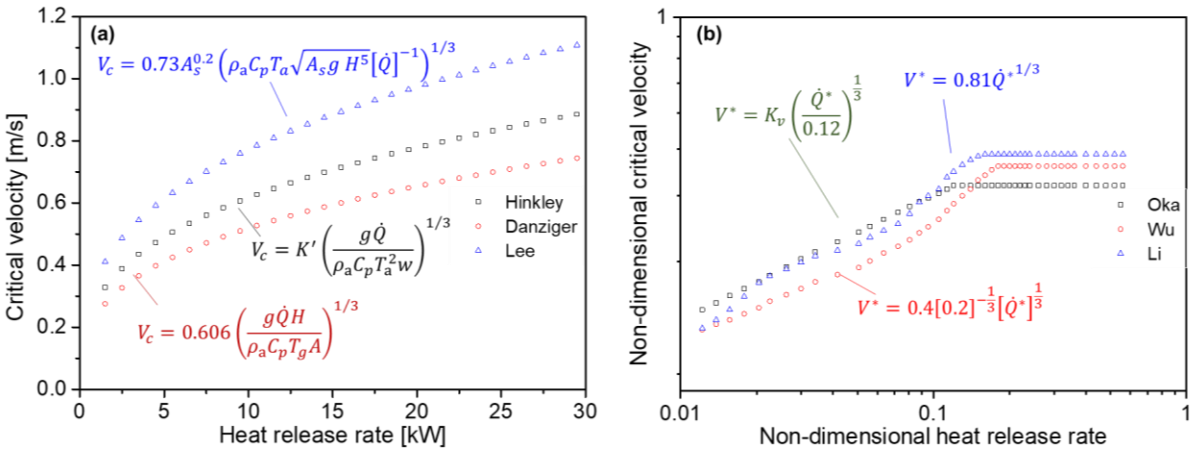

Fig. 9. Predicted results based on proposed empirical correlations (Danziger and Kennedy, 1982; Hinkley, 1970; Lee and Ryou, 2005; Li *et al*., 2010; Oka and Atkinson, 1995; Wu and Bakar, 2000).

3.5. Back-layering length

The back-layering is generally defined as a phenomenon in which smoke flows in the direction of ventilation despite the operation of fans, and it has a negative effect on refugees. However, smoke stratification downstream of the fire source may be disrupted in most tunnel fire scenario when the ventilation velocity approached critical velocity. A lower ventilation rate called "confinement velocity" was introduced to prevent the smoke backflow at a certain distance and to keep certain stratification (Vauquelin and Telle, 2005). The relationship between back-layering length (L_b) and ventilation velocity (V) has been widely studied (Chow *et al*., 2015; Deberteix *et al*., 2001; Li *et al*., 2010; Thomas, 1958; Vantelon *et al*., 1991) considering different parameters, including *Ri*, HRR, and dimensions. The schematic diagram for the back-layering phenomenon was illustrated in Fig. 8.

Thomas (1958) proposed the concept of back-layering for the first time and modified the Froude number to consider the effect of friction resistance on the smoke back-layering distance. Vantelon *et al*. (1991) suggested the dimensionless back-layering distance as 0.3 times of the Richardson number. Deberteix *et al.* (2001) carried out a set of fire tests in a model of the Paris metro and claimed a linear relationship between dimensionless back-layering length and 1/3 power of the Richardson number. However, in this model, the back-layering length was given as a negative value when the HRR was zero.

Li *et al.* (2010) proposed equations to calculate the dimensionless back-layering length based on model scale tests. Chen *et al.* (2015) and Tang *et al*. (2016) modified the equations proposed by Li *et al.* (2010) considering the combination of ceiling extraction system and longitudinal ventilation system, and the relative position of the vent and the fire source. Zhang *et al.* (2016) also prosed a model to predict the back layering length including the factor of blockage ratio metro train length. Based on a large number of experiments, various equations were proposed to calculate the dimensionless back-layering distance (Chow *et al*., 2015; Guo *et al*., 2019). Tables 12 and 13 show the general information of these experimental tests and the empirical equations developed, respectively.

Table 12. Tests and data related to the back-layering length, where L_b and H_{sh} are the back-layering length and shaft height, respecitvely.

Parameters	Length [m]	Height [m]	Width [m]	Aspect Ratio	Fire source [kW]	Ventilation [m/s]	L_b (H_{sh}) [m]
Channel dimensions (Vauquelin, 2005)	10	0.25	0.5	2	Air and Helium 0.1-10	-	-
Ventilation effect (Ingason and Zhen, 2010)	10 (±20°)	0.3	0.4	1.33	Wood crib 0-110	0.33-0.87	0.15 ~ 2.2
Critical velocity (Li *et al.*, 2010)	12	0.25	0.25	1	0.7-16.7	-	-
		0.393	0.45	0.11	2-18.4		-
Ventilation velocity, T, and $\dot{q}''$ (Fan et al., 2016)	-	0.25	0.3	1.2	Heptane 155 ~ 215 63 ~ 106.8 145 ~ 172	0 ~ 0.67	0 ~ 0.25
		0.25	0.45	1.8			0 ~ 0.25
		0.25	0.6	2.4			0.5 ~ 0.75
		0.4	0.3	0.75			0.5 ~ 0.75
		0.4	0.45	1.125			2.5 ~ 2.25
		0.4	0.6	1.5			> 3.75
Velocity (Wang *et al.*, 2018)	72	1.3	1.5	1	LPG 30, 40, 50	NVS 0.3, 0.5	7-20
Ambient pressure, w/o train blockage (Wu *et al.*, 2018)	12	0.5	0.25-0.45	0.5-0.9	Propane, 40-160	0.4-0.7	0-2.5
Natural ventilation, large ceiling openings (Guo *et al.*, 2019)	20.8	0.5	1.2	2.4	Heptane, 6.9	NVS	5.8-8.5 (0)
					25.8		5.2-5.8 (0.35)
					49		5-5.2 (0.5)
					57.6		4-5 (0.65)
					159		3.2-4.3 (0.8)

Table 13. Derived formulas for investigating back-layering distance

Authors	Smoke back-layering distance	Comments
Thomas (1958)	$L_b^* = \frac{L}{H} \propto \frac{1}{Fr} = \frac{gH\dot{Q}}{\rho_a c_p T_{sm} V^3 A}$	
Vantelon *et al.* (1991)	$L_b^* \propto Ri'^{0.3}$	$Ri' = \frac{g\dot{Q}}{\rho_a c_p T_a V^3 H}$
Deberteix *et al.* (2001)	$L_b^* = 7.5(Ri^{\frac{1}{3}} - 1)$	$Ri = \frac{gD\Delta T}{T_a V^2}$
Hu *et al.* (2008)	$L_b = \ln\left[K_2\left(\frac{C_K H}{V^2}\right)\right]/0.019$	C_K 0.2-0.4, $K_2 = g\gamma\left(\dot{Q}^{*\frac{2}{3}}/Fr^{\frac{1}{3}}\right)^{\varepsilon}$ $Fr = V^2/gH_{ef}$ $\dot{Q}^{*\frac{2}{3}}/Fr^{\frac{1}{3}} < 1.35, \gamma = 1.77, \varepsilon = \frac{6}{5}$ $\dot{Q}^{*\frac{2}{3}}/Fr^{\frac{1}{3}} > 1.35, \gamma = 2.54, \varepsilon = 0$
Ingason *et al.* (2010)	$L_b^* = 17.3\ln(0.4/V^*)$	$V^* = V/\sqrt{gH}$
Li *et al.* (2010)	$L_b^* = \begin{cases} 18.5\ln\left(\frac{0.81\dot{Q}^{*\frac{1}{3}}}{V^*}\right), & \dot{Q}^* \le 0.15 \\ 18.5\ln\left(\frac{0.43}{V^*}\right), & \dot{Q}^* > 0.15 \end{cases}$	$V^* = \frac{V}{\sqrt{gH}}$ $\dot{Q}^* = \dot{Q}/(\rho_a c_p T_a g^{1/2} H^{5/2})$
Chow *et al.* (2015)	$L_b = -\frac{1}{K} ln\left[\frac{V^2}{gh}\frac{1}{\gamma(\dot{Q}^{*2/3}/Fr^{1/3})^{\varepsilon}}\right]$	

Weng *et al.* (2015)	$L_b^* = 7.13\ln\left(\frac{\dot{Q}^*}{V^{*3}}\right) - 4.36$	$V^* = \frac{V}{\sqrt{gH}}$ $\dot{Q}^* = \dot{Q}/(\rho_a c_p T_a g^{1/2}\bar{H}^{5/2})$
Chen *et al.* (2015)	$L = \begin{cases} 18.5H\ln\left(0.81Q^{**1/3}/v^{**}\right), & Q^{**} \le 0.15 \\ 18.5H\ln(0.43/v^{**}) & Q^{**} > 0.15 \end{cases}$	effect of ceiling extraction upstream $Q^{**} = \frac{\dot{Q}_0 - c_p VS\Delta T_{max} e^{-\frac{\alpha D}{c_p \dot{m}}d}}{\rho_0 c_p T_0 g^{\frac{1}{2}} H^{\frac{5}{2}}}$ $v^{**} = \frac{v + \rho VS/2A\rho_0}{\sqrt{gH}}$
Zhang *et al.* (2016)	$L_b^* = \begin{cases} \frac{L_b}{H} = 6.956\ln\left(\frac{1.712\dot{Q}^{*\frac{1}{3}}}{V^*/(1-\varphi)}\right), \dot{Q}^{*\frac{1}{3}} \le \dot{Q}_{L=L_T}^{*1/3} \\ \frac{L_T}{H} + 19.342\ln\left(\frac{0.935\dot{Q}_{b-T}^{*1/3}}{V^*}\right), \dot{Q}^{*\frac{1}{3}} > \dot{Q}_{L=L_T}^{*1/3} \end{cases}$	$\dot{Q}_{L=L_T}^{*\frac{1}{3}} = \frac{0.584 \cdot V^*}{(1-\varphi)}\exp\left(\frac{\frac{L_T}{H}}{6.956}\right)$ L_T metro train length (m) $\dot{Q}_{L=L_T}^*$ Critical dimensionless HRR $\dot{Q}_{b-T}^*$ dimensionless HRR of virtual fire source at the rear of metro train

3.6. Smoke layer thickness

Fig. 6(d) shows the schematic diagram of the smoke layer thickness. The determination of the smoke layer thickness plays a vital role in fire safety engineering as it affects the occurrence of plug-holing phenomena, fan performance adjustment, and tunnel geometry effect. Cooper *et al.* (1982) proposed a method named N-percentage rule to distinguish the interface between the layers of smoke and fresh air. However, it is tricky for the choosing of the value N, and it is inapplicable for cases where the gas at the lower part of an enclosed space is heated to be higher than the ambient temperature. Jassens *et al.* (1992) proposed to use the height of the smoke layer interface Zi, which can be adjusted with the vertical temperature. Gao *et al.* (2016) conducted model scale tests and proposed the buoyancy frequency method to estimate the smoke layer thickness. However, all above methods can only be used to determine the interface between the smoke layer and ventilation airflow based on temperature vertical distribution. To predict the smoke layer thickness, Xu *et al.* (2019) proposed an empirical equation based on a set of scaled model tests with nature ventilation condition. Table 14 summarizes all methods for calculating the smoke layer thickness.

Table 14. Derived formulas for investigating smoke layer thickness.

Authors	**Proposed formulas**
Cooper *et al.* (1982)	$T_i - T_a = (T_{max} - T_a)N/100 \quad (10 < N < 30)$
Jassens *et al.* (1992)	$Z_i = \frac{T_a(I_1 I_2 - H^2)}{I_1 + I_2 T_a^2 - 2T_a H}, \quad I_1 = \frac{H - Z_i}{T_u} + \frac{Z_i}{T_a} = \int_0^H \left(\frac{1}{T(z)}\right) dz$ $I_2 = \frac{H-Z_i}{T_u} + Z_i T_a = \int_0^H (T(z))dz, \quad N = 100(T(Z_i) - T_1)/(T_u - T_i)$
He *et al.* (1998)	$r = r_u + r_l, \quad r(H_i) = \min(r_t)$ $r_u = \frac{1}{(H - H_i)^2}\int_{H_i}^{H} T(z)dy \int_{H_i}^{H} \frac{1}{T(z)}dy, \quad r_l = \frac{1}{H_i^2}\int_0^{H_i} T(z)dy \int_0^{H_i} \frac{1}{T(z)}dy$
Gao *et al.* (2016)	$N_L = \left(-gT_a \frac{\partial(1/T)}{\partial z}\right)^{1/2}$
Xu *et al.* (2019)	$d = 1.24\left(\frac{\dot{m}_{sm}}{(w/H)^2}\right)^{1/3} - 0.13 \quad$ (natural ventilation)

3.7. Plug-holing

Natural Ventilation System (NVS) has been widely adopted in tunnels due to high cost-effectiveness. However, this type of system may not be applied to all scenarios affecting by fire size, HRR, tunnel and shaft cross-section areas, and hydraulic diameter. Particularly, when the lower fresh air layer mixes with the upper smoke layer, the plug-holing phenomenon occurs near the shaft region, as shown in Fig. 10.

However, very limited studies have been carried out in this area until the recent 10 years, such as Ji. *et al.* (2012) and Beak *et al.* (2017) (see Fig. 5). In their method, the Froude number and the Richardson number were modified as the ratio of inertia force over the smoke and buoyancy force of vertical shaft, and the ratio of buoyancy force of vertical shaft over inertia force of smoke, respectively. Hinkley (1970) also proposed a method of using modifying the Froude number to identify this phenomenon without considering the effect of the geometry of a shaft, which was further considered by Spratt *et al.* (1974). However, the effect of the position of the vertical shaft was not taken into account in previous studies except in a test conducted by Takeuchi *et al.* (2017) using a 1:20 scale tunnel model.

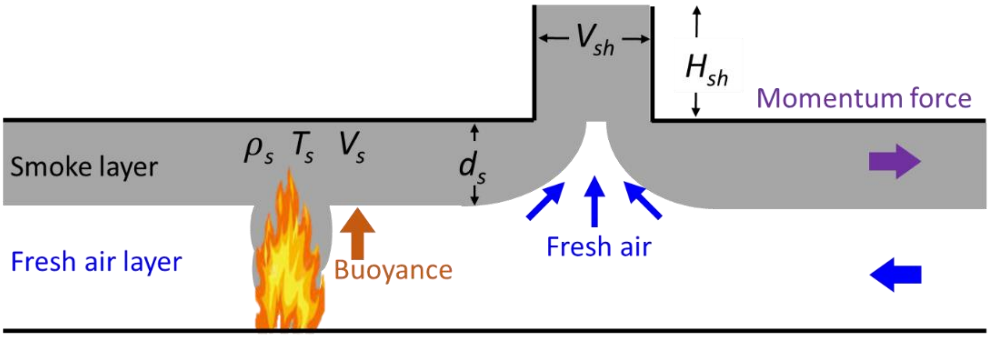

Fig. 10. Conceptual diagram of the plug-holing phenomenon

Thus, the new determine the occurrence of the phenomenon considering the effect of the vertical shaft (J. Ji *et al*., 2012). Table 15 summarizes the studies on the plug-holing phenomenon focusing on the criterion of identifying the occurrence of this phenomenon. The main information and correlation of the experimental data is shown in Table 16.

Table 15. Data experimented to investigate the plug-holing phenomena

Parameters	Length [m]	Depth [m]	Aspect Ratio	w_{sh} [m]	D_{sh} [m]	H_{sh} [m]	Fire source [kW]	Ventilation condition
Shaft height (J. Ji *et al.*, 2012)	6	2	-	0.3	0.3	0 - 1	Methanol 7-53	NVH
Cross-section AR, HRR (Baek *et al.*, 2017)	7	0.3 - 0.54	0.56-1	0.15	0.06	0.1-0.18	n-Heptane 1.2 - 10.1	NVH
Location of vertical shaft (Takeuchi *et al.*, 2017)	5	0.5	-	-	-	0.06, 0.25	Propane 1.5 - 4.4	NVH
Exhaust vent (Jiang *et al.*, 2018a)	22	0.6	-	7.5 (vent)	20 (vent)	-	Methanol 2.8-16.8	Exhaust vent

Table 16. Criteria of critical number and empirical correlations for plug-holing phenomenon

References	Critical Number	Non-dimensional analysis	Conditions
Hinkley (1970)	Ri < 1.8	$\frac{\Delta\rho g H_{sh} A_{sh}}{\rho_{sm} V_{sm}^2 d_{sm} w_{sh}}$	Simple vents without chimney effect in a shopping mall, where the effect of the tunnel shape was not a parameter
Ji *et al.* (2012)	Ri < 1.4	$\frac{\Delta\rho g H_{sh} A_{sh}}{\rho_{so} V_{sm}^2 d_{sm} w_{sh}}$	Small-scale tunnel for considering the effect of HRR and the height of natural ventilation. ρ_{so} density of smoke without smoke exhaust

Baek *et al.* (2017)	Fr > 2.75	$\frac{\rho_{sm}V_c^2 d_{sm}w}{\rho_a g H_{sh}(\frac{1}{T_a}-\frac{1}{T_{sm}})d_{sh}w_{sh}}$	Small-scale tunnel for considering the effect of HRR and the aspect ratio of tunnel d_{sh} depth of shaft
Takeuchi *et al.* (2017)	Ri < 0.3	$\frac{\Delta\rho g H_{sh}A_{sh}}{\rho_{sm}V_{sm}^2 d_{sm}w}$	Effect of vertical shaft location for distinguish the occurrence of plug-holing
Jiang *et al.* (2018a)	Fr < 1.8	$\frac{V_{sm}A_{sh}}{(\frac{g\Delta T}{T_a})^{1/2}{d_{sm}}^{5/2}}$	Experimental study under the exhaust vent

4. Application of machine learning on tunnel fires

The growing number of underground tunnels inevitably increases the risk of tunnel fire incidents. To reduce the frequency of massive fire accidents in tunnel and the damage caused by fire, it is necessary to discover the fire incident as quickly as possible (Muhammad *et al*., 2018). The earlier sensing technologies were primarily based on point sensors for heat, gas, flame, and smoke flows. Very limited studies have been conducted on tunnel fire detection using AI methods. Xue (2010) built up a three-layer ANN to identify the fire in tunnels using the information of temperature smoke density and density of CO measured by sensors. The neural network was trained using numerical simulation results. The accuracy, generalization ability, and correct recognition rate were demonstrated. The application of ANN in detecting tunnel fire is promising. In our previous work (Wu et al., 2020a, 2020b), AI method successfully identified the fire source and predicted the fire evolution in tunnel. A LSTM-RNN model and a large CFD dataset of tunnel fire were adopted to train the smart system.

Today, various types of fire detection technologies have been adopted for tunnel fire safety, such as remote monitoring, high-resolution sensor, thermal imaging, and data-driven high-performance computing (Jevtić and Blagojević, 2014). Particularly, as cameras are often installed to monitor the situation inside the tunnel, ideally, these real-time images can quickly detect and continuously monitor the fire (Gaur *et al*., 2020). However, their reliability is still questionable, because of (1) poor image quality caused by the low visibility in the tunnel and low camera contrast, and (2) scene complexity due to moving cars and lights. Han and Lee (2009; 2007) used consecutive images captured by video and then separated fire flame from the lights in tunnels using edge slop density function and then removed the noises in images using the median filtering method to detect fire. They also realized the real-time detection of tunnel fire and smokes by image processing techniques, including movement detection, edge detection, and color information. Today, the smart firefighting system is an emerging fire research area, but it is still far from mature for real applications in tunnel. For any smart fire engineering system, a sufficient and reliable database is required to reduce the false alarm and provide reasonable fire forecast (Grant et al., 2015; Wu et al., 2020a), and the prospective of using this database in smart firefighting is illustrated in Fig. 10.

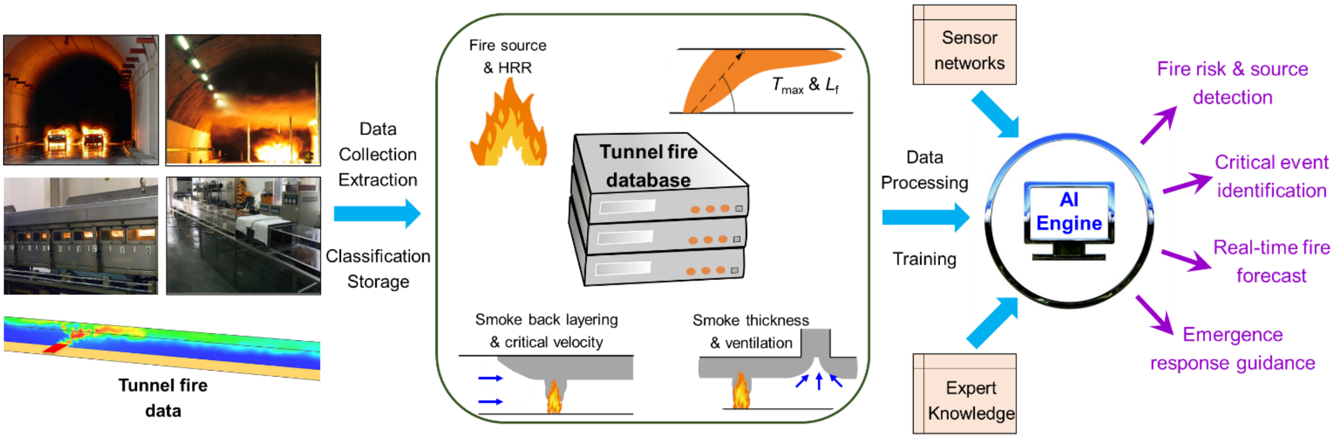

Fig. 10. The prospective of using this database for smart firefighting in tunnel.

4.1. Database establishment

Big data features in three aspects: volume, variety, and velocity (Chi *et al*., 2016). To enable the training of AI models in engineering applications, forming an organized database is the first step. Due to its complex nature, it is still challenging to properly store, manage, maintain, and analyze a big database. In general, the establishment of the database is a multi-step task, that is,

(1) Data collection: search all available literature and extract all useful data from these documents,

(2) Data preprocessing: remove outliers, data quality check, remove noises, and filtering, and

(3) Data mining: extract valuable information.

Herein, we propose a framework to organize all available data of fire engineering into a standard format. As a demonstration, the established tunnel-fire database in this work is publicly available on Github: https://github.com/PolyUFire/Tunnel_Fire_Database.

Data collection. For a typical fire test or numerical fire simulations, a number of parameters are commonly measured (see Table 4), and the data can be classified into two main categories,

(I) Sensor data: such as the temperature by thermocouples or other heat detectors, the presence of smoke by smoke detectors, CO and CO_2 by gas detectors, and heat flux by a radiometer or plate thermometer. Sensors are often installed at one or many locations for long-term measurement. In other words, sensor data are often time sequences of point or line measurements, which have both spatial and temporal dimensions.

(II) Visual data: such as the video from CCTV and infrared (IR) cameras, and satellite images (in large-scale urban and wildland fires). For numerical simulations, the visual data refer to the contours and videos generated from computational results. These time-sequence image data can directly show the real-time scene and scale of the fire, evacuation process, distributions of smoke and temperature, and firefighting activities. Compared to sensor data, the visual data are 2-D or 3-D in nature that are several orders of magnitude larger.

Based on the data available, there are two AI methods, i.e., sensor-based method and vision-based method. Today, most of the existing fire research only provide the limited and processed sensor data in the report and publication. Often, only selected data are presented in the form of plots, while the raw measurement data are not listed in the table or documented available to the public. Comparatively, the video data are even rare, due to the large data size and complexity in the further data processing.

Currently, the database can only be established with all available sensor data that can be accessed online, such as journal publications and technical reports. A thorough literature review is required to feed the database. For example, Sections 2 and 3 demonstrate the process of literature review, and all documents were categorized into seven key parameters, namely, flame length, maximum temperature, smoke layer thickness, critical velocity, back-layer length, and plug-holing. After then, all related experimental data were extracted from these documents. To enforce a convenient data search, all raw images in the original documents are presented with a detailed description of data.

Data mining and sharing. Since the fire process is generally complex and influenced by multiple factors, it is essential to provide adequate test information before the data process. Because most of the existing fire test data initially are not produced and presented under the principle of sharing, it is extremely challenging to extract all the necessary information and data from the accomplished and on-going tests, as well as to make a fair comparison among existing data.

4.2. Framework of fire database

To maximize the usage of valuable existing data and facilitate the database establishment of future fire tests, we propose a **framework and guideline** for data collection in fire tests. Using the tunnel fire test as an example, the data collection should include:

1) ***Structure and test information***. Studies should report the basic settings of the fire tests, including the

scaling factor, tunnel size, ventilation system, tunnel construction material, and on-site weather conditions (ambient temperature, humidity, and wind).

2) ***Fire information***. Fire location, fire geometrical dimension, components of combustible material, amount of burning materials should be given.
3) ***Sensor information***. Apart from the arrangement of all the sensors and other measuring devices, more information on sensor type, measuring range, delay time, and frequency or interval of data collection need to be provided.
4) ***Special-temporal sensor data***. The measured data obtained from sensors during whole stages of fire, including pre-fire ignition, fire development, decay, and firefighting should be provided.
5) ***Video data***. The fire phenomena should be recorded by various video cameras. All video data should include a detailed description of the location, environmental and personal information, and time sequence of different fire processes and critical events, such as the ignition, fire spread, ventilation, and suppression.
6) ***Imperfection data***. Some researchers prefer not to provide imperfect data due to the unnormal measurement, missing, or other reasons. However, it is highly encouraged to provide all data, because those data not only could be treated with technics, such as filling and filtering, but also provide crucial experiences for other researchers and future tests.

Once the raw data are collected and documented, it is crucial to analyze the data by utilizing preprocessing methods. Measuring devices, human factors, and fire impacts may cause noises, redundancies, and outliers to the data collected. Thus, those collected data need to be inspected and processed. With the limited amount of experimental data in the literature, the experimental data were directly extracted from the available documents, and no further processing was conducted to guarantee the authenticity of the database. The procedure of the database generation follows:

1) Extract all available basic information based on the proposed data collection framework,
2) Extract testing results in the form of a table, figure, and supplemental material, and
3) Organize extracted data of various sources into tables with consistent data format and metadata.

Take the current database of flame length in tunnel fire as an example. Information related to the tunnel and fire data were first extracted from the literature, as listed in Table 6. Then, individual results of the flame length were acquired from the authors of the literature or extracted from plots one by one. Afterward, form the database of flame length by giving a table composed of eleven columns from left to right, showing the scaling factor of the tests, the HRR of fire, tunnel length, width and height, the velocity of wind in the tunnel, the type of the combustible material, the location of the fire, the measured flame length, the related reference, and comments, respectively. The last two columns served to further check the data source. Each row of the table describes a testing data point extracted from the corresponding source. Note that not all the information illustrated in the guideline was extracted for the database. It is mainly because lots of information is missing for most of these documents. Thus, it is important and urgent for researchers to have a standard guideline to present their scientific findings, and it should also be a community effort to enforce the data collection and improve the guideline.

Essentially, the data stored in the current database served as the first step for further studies. More valuable results can be gained by analyzing these data. For instance, the distribution of temperature in the tunnel can be recognized from the sensor data that were measured at various locations. Similarly, the shape and motion of the fire flame and smoke could be approximately identified by analyzing the time series data of temperature. The database also provides a macroscopic overview of all studies achieved and to be achieved.

The review of the current database further reveals a critical problem, that is, most of the literature **only reports steady-state quantities**, such as HRR, temperature profiles, ventilation condition, and smoke layers, because these steady-state values are easy to report, analyze, and extrapolate. For any fire process, there is a transient process before any steady state could be achieved. Although most of these transient raw data are recorded during the tests, these data were rarely documented, analyzed, and presented to the fire community. It is mainly because the amount of these transient data is tremendous, and they are difficult to analyze and visualize and cannot provide useful engineering correlations like those in Tables 5, 7, 8, 10, 12, and 14 for steady-state values. Consequently, the community is still lack of knowledge about the time scale for fire development and critical events in the tunnel and other structures. Therefore, the data collection and documentation for transient fire processes are significantly important to achieve any capacity of fire forecast. Also, studies and data on fire spread in tunnels are in high demand, because most of the existing fire tests use the fixed fire sources. The overview points out the potential research directions in future tunnel fire tests.

4.3. A case study on tunnel fire forecasting

In this section, an example is given to illustrate the application of machine learning on tunnel fire safety engineering using a big database. Here, no expertise knowledge of the critical velocity is input to the AI model before training. A conventional multilayer perception (machine-learning) model is established to predict the critical velocity in a tunnel considering multiple factors related to tunnel dimension and HRR. The Python code and the database used for predicting the critical velocity is also open access in Github.

As a demonstration, the database is generated from four empirical equations in Table 11 (Li *et al*., 2010; Tang *et al*., 2018b; Weng *et al*., 2015; Wu and Bakar, 2000). Note that these empirical equations were fitting correlations, so that they essentially represent a large amount of experimental data. Fig. 12 shows the parameters influencing the critical velocity considered in previous studies, that is, length, width and height of the tunnels, hydraulic diameter, and HRR. The tunnel geometries and the range of HRR listed in Table 17 are from available tunnel fire tests. Hydraulic diameter describing the characteristic length of tunnel can be calculated with the tunnel dimensions. It should be noted that for the second series of test conducted by Li *et al.* (2010), tunnel height is regarded as characteristic length. One series of the values of these parameters produces one training sample. To enrich the training of database with all available data, more training samples can be generated by interpolation between the range of these parameters. An interval of 0.05 kW was adopted for all the tests. Finally, a database including 3,482 training samples was formed.

Table 17. General information and parameters of tunnels for demonstration.

References	L [m]	w [m]	H [m]	D_H [m]	$\dot{Q}$ [kW]	$\dot{Q}$ interval [kW]
Wu *et al*. (2000)	15	0.136	0.25	0.176	1.5-30	0.05
		0.25	0.25	0.25		
		0.5	0.25	0.333		
		1	0.25	0.4		
Li *et al*. (2010)	12	0.25	0.25	0.25	0.7-16.7	
		0.45	0.393	0.393	2-18.4	
Weng *et al*. (2015)	15	0.48	0.54	0.508	1.59-12.38	
Tang *et al*. (2018b)	8	0.34	0.44	0.384	1.5-18	

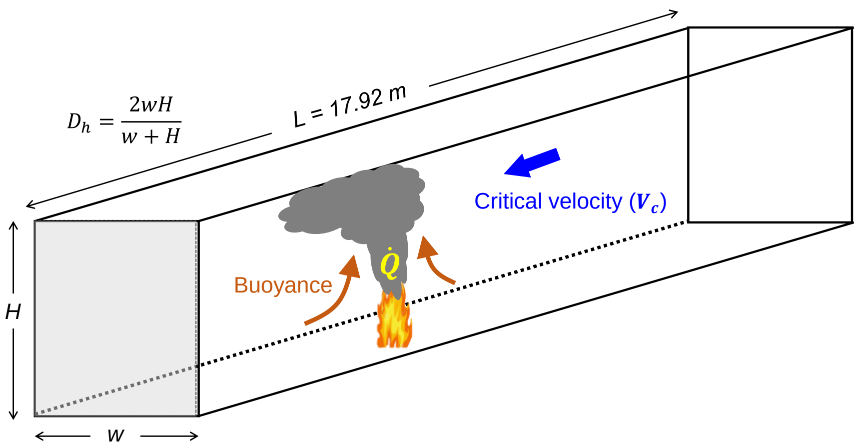

Fig. 12. Parameters of the tunnel for demonstration.

Fig. 13 illustrates the generation of the training database. The raw dataset was stored in a matrix, in which the columns represent the parameter information, and the rows represent the varieties of these parameters in each case. Each case was labeled the actual value of critical velocity calculated from equations in Table 9. The labels are individually normalized to make them have the same range between 0 and 1 with the min-max normalization function (Komer *et al*., 2014). It is to avoid the condition that the features having more extensive ranges would dominate the computation of similarity (Aksoy and Haralick, 2001). Then, labeled cases were randomly divided into training, validation, and test sets with a ratio of 0.6, 0.2, and 0.2, respectively. The training dataset was utilized for training the ANN model.

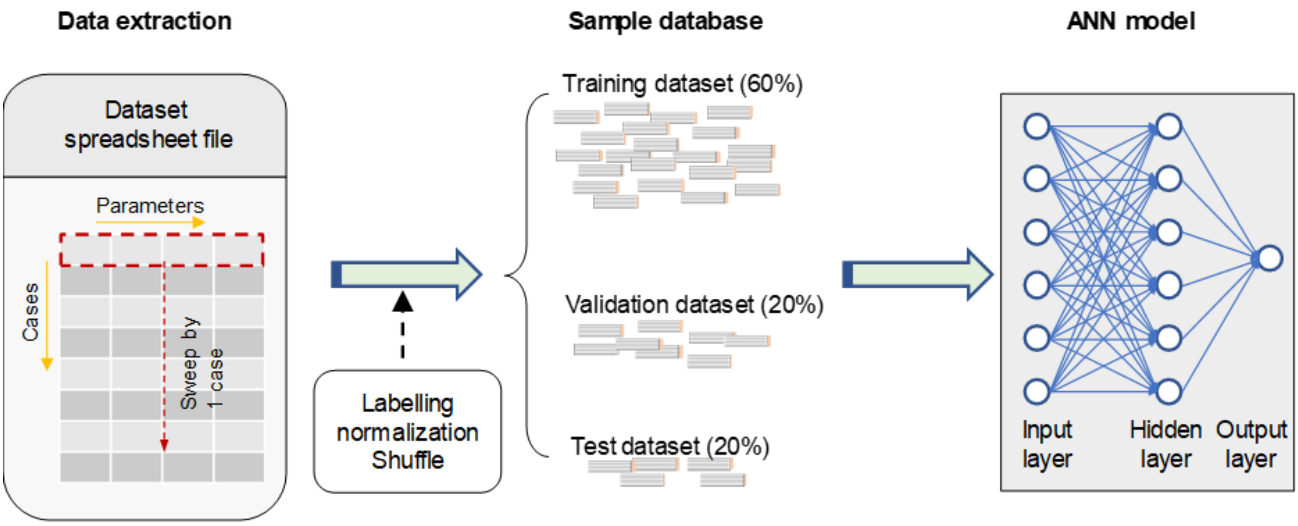

Fig. 13. Establishment of database and training of the ANN model.

Fig. 14 shows the architecture of the 3-layer ANN model adopted in this study. The first two layers each have 6 neurons, which is equal to the number of parameters. The neuron in the output layer gives the prediction of the critical velocity. Nonlinear activation function "Tanh" is adopted for each layer. The whole model was trained by minimizing the loss function of mean squared error (MSE). The optimizer "adam" was chosen to tie together the coefficients to be updated and the loss function. Note that alternative loss functions, activation functions, and optimizers can also be adopted if applicable. The coefficient of determination R^2 was adopted for the evaluation of the trained model. R^2 is a scale-free parameter, meaning that it is independent of the exact differences of predictions, and the performance of models can be directly evaluated compared with this value.

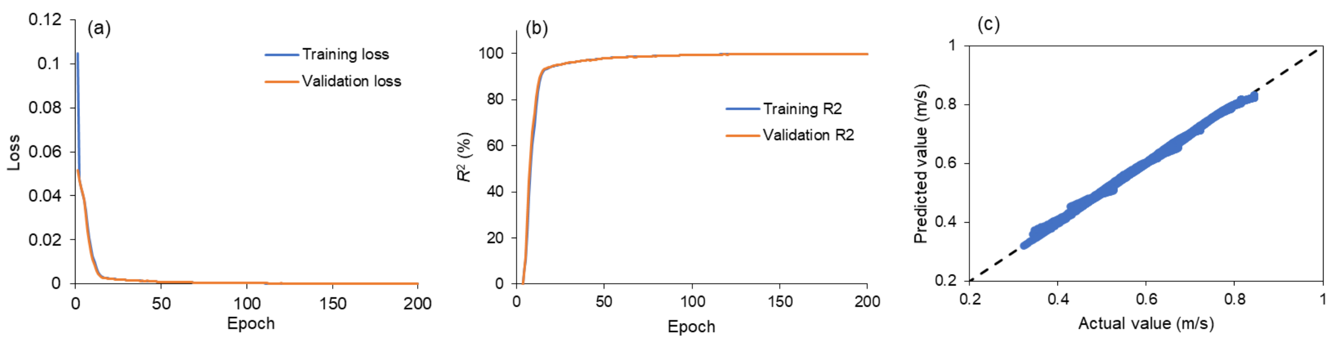

Fig. 14. The variations of (a) loss, and (b) R^2 during the training process, and (c) Comparison between predicted and actual values

Fig. 14(a) shows the evolvements of the loss function. As expected, the loss of the model decreases drastically with training epochs. After training for 20 epochs, the model has already converged with a loss of 6e-5, which demonstrates the sufficiency of the pre-set training epoch number of 100. The validation loss shows a similar trend with the training loss. No overfitting phenomenon was observed in this study, which could be attributed to the simplicity of the current predicting task. Fig. 14(b) shows the evolvement of R^2 with the increase of epochs. Both the training and validation R^2 attained a value approaching 100 soon after training. After a slight fluctuation at an early stage, R^2 kept almost unchanged at 99.99%. Fig. 14(c) compares the predicted and actual value of critical velocity in tunnels. All the data points align with the diagonal line, showing the excellent performance of the trained ANN model in the prediction of critical velocity. Though this case study is simple, the capability of artificial intelligence methods in solving problems related to fire safety engineering has been demonstrated.

5. Conclusions

In light of the recent advances in big data and artificial intelligence, this paper aims to establish a database that contains all existing experimental data of tunnel fire, based on an extensive literature review on tunnel fire tests. This database summarizes seven key quantities of tunnel fire, namely, heat release rate, flame length, maximum ceiling temperature, smoke layer thickness, critical ventilation velocity, back-layering length, and plug-holing. This database is open access at GitHub. The test conditions, experimental phenomena, and data of each literature work were organized and categorized in a standard format that could be conveniently accessed and continuously updated. Based on this database, machine learning is applied to successfully predict the critical ventilation velocity of a tunnel fire as a demonstration.

The review of the current database reveals more valuable information and hidden problems in the conventional collection of test data. In general, the existing data on tunnel fire research is still not sufficient to form a reliable database in support of smart firefighting. Particularly, the video data, imperfect data, and transient data are lacking, and there is no standard procedure to collect and organize the data in the fire community. This review proposes a framework and guideline for data collection in future tunnel fire research. The established database and methodology will promote the application of artificial intelligence and smart firefighting in tunnel fire safety.

Acknowledgments

This work is funded by the Hong Kong Research Grants Council Theme-based Research Scheme (T22-505/19-N) and the PolyU Emerging Frontier Area (EFA) Scheme of RISUD (P0013879). The authors also thank Mr. Ao Li (PolyU) and other SureFire members for valuable comments.

References

AIPCR, 1999. Fire and Smoke Control in Road Tunnels, Association Internationale Permanente des Congrès de la route, http://www.piarc.org.

Aksoy, S., Haralick, R.M., 2001. Feature normalization and likelihood-based similarity measures for image retrieval. Pattern Recognition Letters 22, 563–582. https://doi.org/10.1016/S0167-8655(00)00112-4

Alpert, R.L., 1975. Turbulent Ceiling-Jet Induced by Large-Scale Fires. Combustion Science and Technology. https://doi.org/10.1080/00102207508946699

ANDERSON, D., 1936. THE CONSTRUCTION OF THE MERSEY TUNNEL.(INCLUDES PHOTOGRAPHS). Journal of the Institution of Civil Engineers 2, 473–516.

Association, N.F.P., 2011. NFPA 502, Standard for road tunnels, bridges, and other limited access highways. NFPA.

Atkinson, G.., Wu, Y., 1997. Short Control in Sloping Tunnels. Fire Safety Journal 27, 335–341.

Baek, D., Sung, K.H., Ryou, H.S., 2017. Experimental study on the effect of heat release rate and aspect ratio of tunnel on the plug-holing phenomena in shallow underground tunnels. International Journal of Heat and Mass Transfer 113, 1135–1141. https://doi.org/10.1016/j.ijheatmasstransfer.2017.06.044

Barbato, L., Cascetta, F., Musto, M., Rotondo, G., 2014. Fire safety investigation for road tunnel ventilation systems – An overview. Tunnelling and Underground Space Technology incorporating Trenchless Technology Research 43, 253–265. https://doi.org/10.1016/j.tust.2014.05.012

Beard, A., Carvel, R., 2012. Handbook of tunnel fire safety. ICE Publishing.

Beard, A.N., 2009. Fire safety in tunnels. Fire Safety Journal 44, 276–278. https://doi.org/10.1016/j.firesaf.2008.06.008

Bendelius, A., Rhodes, N., Abellam, A., 2007. Systems and Equipment for Fire and Smoke Control in Road Tunnels. World Road Association, Paris.

Bettelini, M., Riess, I., Ingenieur-gmbh, R., 2016. Progress in tunnel ventilation - the Mont Blanc tunnel Progress in Tunnel Ventilation – The Mont-Blanc Tunnel.

Blennemann, F., Girnau, G., 2005. Fire Protection in Vehicles and Tunnels for Public Transport. STUVA, Köln, Mai.
Blinov, V.I., 1957. Certain laws governing the diffusive burning of liquids. Academiia Nauk, SSR Doklady 113, 1094–1098.
Blinov, V.I., Khudiakov, G.N., 1961. Diffusion Burning of Liquids. U.S Army Enginner Research and Development Laboratories.
Cao, Y., Yang, F., Tang, Q., Lu, X., 2019. An attention enhanced bidirectional LSTM for early forest fire smoke recognition. IEEE Access 7, 154732–154742. https://doi.org/10.1109/ACCESS.2019.2946712
Carvel, R., 2019. A review of tunnel fire research from Edinburgh. Fire Safety Journal 105, 300–306. https://doi.org/10.1016/j.firesaf.2016.02.004
Casey, N., 2020. Fire incident data for Australian road tunnels. Fire Safety Journal 111, 102909. https://doi.org/10.1016/j.firesaf.2019.102909
Chaabat, F., Salizzoni, P., Creyssels, M., Mos, A., Wingrave, J., Correia, H., Marro, M., 2020. Smoke control in tunnel with a transverse ventilation system : An experimental study. Building and Environment 167, 106480. https://doi.org/10.1016/j.buildenv.2019.106480
Chen, C., Xiao, H., Wang, N., Shi, C., Zhu, C., Liu, X., 2017. Experimental investigation of pool fire behavior to different tunnel-end ventilation opening areas by sealing. Tunnelling and Underground Space Technology incorporating Trenchless Technology Research 63, 106–117. https://doi.org/10.1016/j.tust.2017.01.001
Chen, L., Mao, P., Zhang, Y., Xing, S., Li, T., 2020. Experimental study on smoke characteristics of bifurcated tunnel fire. Tunnelling and Underground Space Technology 98, 103295. https://doi.org/10.1016/j.tust.2020.103295
Chen, L.F., Hu, L.H., Zhang, X.L., Zhang, X.Z., Zhang, X.C., Yang, L.Z., 2015. Thermal buoyant smoke back-layering flow length in a longitudinal ventilated tunnel with ceiling extraction at difference distance from heat source. Applied Thermal Engineering 78, 129–135. https://doi.org/10.1016/j.applthermaleng.2014.12.034
Cheong, M.K., Cheong, W.O., Leong, K.W., Lemaire, A.D., Noordijk, L.M., 2014. Heat Release Rate of Heavy Goods Vehicle Fire in Tunnels with Fixed Water Based Fire-Fighting System. Fire Technology 50, 249–266. https://doi.org/10.1007/s10694-013-0367-0
Chi, M., Plaza, A., Benediktsson, J.A., Sun, Z., Shen, J., Zhu, Y., 2016. Big Data for Remote Sensing: Challenges and Opportunities. Proceedings of the IEEE 104, 2207–2219. https://doi.org/10.1109/JPROC.2016.2598228
Choi, J., Choi, J.Y., 2016. An integrated framework for 24-hours fire detection. In: Lecture Notes in Computer Science(including subseries Lecture Notes in Artificial Intelligence and Lecture Notes in Bioinformatics).
Chow, W.K., Gao, Y., Zhao, J.H., Dang, J.F., Chow, C.L., Miao, L., 2015. Smoke movement in tilted tunnel fires with longitudinal ventilation. Fire Safety Journal 75, 14–22. https://doi.org/10.1016/j.firesaf.2015.04.001
Chow, W.K., Gao, Y., Zhao, J.H., Dang, J.F., Chow, N.C.L., 2016. A study on tilted tunnel fire under natural ventilation. Fire Safety Journal 81, 44–57. https://doi.org/10.1016/j.firesaf.2016.01.014
Chow, W.K., Wong, K.Y., Chung, W.Y., 2010. Longitudinal ventilation for smoke control in a tilted tunnel by scale modeling. Tunnelling and Underground Space Technology incorporating Trenchless Technology Research 25, 122–128. https://doi.org/10.1016/j.tust.2009.10.001
Cong, H., Wang, X., Kong, X., Xu, H., 2019. Effects of fire source position on smoke extraction efficiency by natural ventilation through a board-coupled shaft during tunnel fires. Proceedings of the Combustion Institute 37, 3975–3984. https://doi.org/10.1016/j.proci.2018.07.015
Cong, H.Y., Wang, X.S., Zhu, P., Jiang, T.H., Shi, X.J., 2017. Improvement in smoke extraction efficiency by natural ventilation through a board-coupled shaft during tunnel fires. Applied Thermal Engineering 118, 127–137. https://doi.org/10.1016/j.applthermaleng.2017.02.092
Cooper, L.Y., Harkleroad, M., Quintiere, J., Rinkinen, W., 1982. An Experimental Study of Upper Hot Layer Stratification in Full- Scale Multiroom Fire Scenarios. Journal of Heat Transfer 104, 741–749.
Cote, A.E., 2008. Fire protection handbook. NationalFireProtectionAssoc.
Danziger, N.H., Kennedy, W.D., 1982. Longitudinal ventilation analysis for the Flenwood canyon tunnels, in: Procedings of the 4th International Symposium of Aerodynamics and Ventilation of Vehicle Tunnels. York, UK, pp. 169–186.
Deberteix, P., Gabay, D., Blay, D., 2001. Experimental study of fire-induced smoke propogation in a tuunel in the presence of longitudnal ventilation. in: Proceedings of the International Conference on Tunnel Fires and Escape from Tunnels, Washington, pp. 257–265.
Ding, H., Quintiere, J.G., 2012. An integral model for turbulent flame radial lengths under a ceiling. Fire Safety Journal 52, 25–33. https://doi.org/10.1016/j.firesaf.2012.03.008
Drysdale, D., 2011. An Introduction to Fire Dynamics, 3rd ed. John Wiley & Sons, Ltd, Chichester, UK. https://doi.org/10.1002/9781119975465
Edith, C., 1996. Science research development. ECSC Steel publications.
Egger, M., 2001. Recommendations of the Group of Experts on Safety in Road Tunnels. UN Economic and Social Council.
Fan, C.G., Ji, J., Gao, Z.H., Sun, J.H., 2013. Experimental study on transverse smoke temperature distribution in road tunnel fires. Tunnelling and Underground Space Technology 37, 89–95. https://doi.org/10.1016/j.tust.2013.04.005
Fan, C.G., Li, Y.Z., Ingason, H., Lonnermark, A., 2016. Effect of tunnel cross section on gas temperatures and heat fluxes in case of large heat release rate. Applied Thermal Engineering 93, 405–415. https://doi.org/10.1016/j.applthermaleng.2015.09.048
Fang, J.., 1973. Analysis of The Behavior of a Freely Burning Fire Quiescent Atmosphere. NBSIR 73-115, National Bureau of Standards, Washington DC.
Feizlmayr, A.H., 1976. Research in Austria on tunnel fire. BHRA. In: Second International Symposium on Aerodynamics and

Ventilation of Vehicle Tunnels. Paper J2, Cambridge, England.
Feng, S., Li, Y., Hou, Y., Li, J., Huang, Y., 2020. Study on the critical velocity for smoke control in a subway tunnel cross-passage. Tunnelling and Underground Space Technology 97, 103234. https://doi.org/10.1016/j.tust.2019.103234
Gao, Z., Ji, J., Wan, H., Li, K., Sun, J., 2015. An investigation of the detailed flame shape and flame length under the ceiling of a channel. Proceedings of the Combustion Institute 35, 2657–2664. https://doi.org/10.1016/j.proci.2014.06.078
Gao, Z., Jie, J., Wan, H., Zhu, J., Sun, J., 2017. Experimental investigation on transverse ceiling flame length and temperature distribution of sidewall confined tunnel fire. Fire Safety Journal 91, 371–379. https://doi.org/10.1016/j.firesaf.2017.04.033
Gao, Z.H., Ji, J., Fan, C.G., Li, L.J., Sun, J.H., 2016. Determination of smoke layer interface height of medium scale tunnel fire scenarios. Tunnelling and Underground Space Technology. https://doi.org/10.1016/j.tust.2016.02.009
Gao, Z.H., Ji, J., Fan, C.G., Sun, J.H., Zhu, J.P., 2014. Influence of sidewall restriction on the maximum ceiling gas temperature of buoyancy-driven thermal flow. Energy and Buildings 84, 13–20. https://doi.org/10.1016/j.enbuild.2014.07.070
Gaur, A., Singh, A., Kumar, Anuj, Kumar, Ashok, Kapoor, K., 2020. Video Flame and Smoke Based Fire Detection Algorithms: A Literature Review. Fire Technology 56, 1943–1980. https://doi.org/10.1007/s10694-020-00986-y
Ghoreishi, 2019. Review of the Punching Shear Behavior of Concrete Flat Slabs in Ambient and Elevated Temperature Mehrafarid 8301–8305.
Giblin, K.A., 1997. Memorial tunnel fire ventilation test program. ASHRAE Journal.
Gong, L., Jiang, L., Li, S., Shen, N., Zhang, Y., Sun, J., 2016. International Journal of Thermal Sciences Theoretical and experimental study on longitudinal smoke temperature distribution in tunnel fires. International Journal of Thermal Sciences 102, 319–328. https://doi.org/10.1016/j.ijthermalsci.2015.12.006
Grant, C., Hamins, A., Bryner, N., Jones, A., Koepke, G., 2015. Research Roadmap for Smart Fire Fighting. NIST Special Publication 1191. https://doi.org/10.6028/NIST.SP.1191
Guo, F., Gao, Z., Wan, H., Ji, J., Yu, L., Ding, L., 2019. Influence of ambient pressure on critical ventilation velocity and backlayering distance of thermal driven smoke in tunnels with longitudinal ventilation. International Journal of Thermal Sciences 145, 105989. https://doi.org/10.1016/j.ijthermalsci.2019.105989
Guo, Q., Zhu, H., Yan, Z., Zhang, Yao, Zhang, Yinping, Huang, T., 2019. Experimental studies on the gas temperature and smoke back-layering length of fires in a shallow urban road tunnel with large cross-sectional vertical shafts. Tunnelling and Underground Space Technology 83, 565–576. https://doi.org/10.1016/j.tust.2018.10.010
Haack, A., 1998. Fire protection in traffic tunnels: general aspects and results of the EUREKA project. Tunnelling and underground space technology 13, 377–381.
Hammarström, R., Axelsson, J., Försth, M., Johansson, P., Sundstrom, B., 2008. Bus Fire Safety Bus Fire Safety, SP report. Research Institute of Sweden, Boras, Sweden.
Han, D., Lee, B., 2009. Flame and smoke detection method for early real-time detection of a tunnel fire. Fire Safety Journal 44, 951–961. https://doi.org/10.1016/j.firesaf.2009.05.007
Hansen, R., 2015. Study of heat release rates of mining vehicles in underground hard rock mines. Malardalen University.
Hasemi, Y., Yoshida, M., Yokobayashi, Y., Wakamatsu, T., 1997. Flame heat transfer and concurrent flame spread in a ceiling fire. Fire Safety Science 5, 379–390.
He, Y., Fernando, A., Luo, M., 1998. Determination of interface height from measured parameter profile in enclosure fire experiment. Fire Safety Journal 31, 19–38.
Heselden, A., Hinkley, P., 1970. Smoke travel in shopping malls. Experiments in cooperation with Glasgow Fire Brigade. Parts 1 and 2. Fire Research Station.
Heselden, A.J.M., 1976. Studies of fire and smoke behaviour relevant to tunnels. Proceedings of the Second International Symposium of Aerodynamics and Ventilation of Vehicle Tunnels, Paper J1.
Heskestad, G., 2016. Fire plumes, flame height, and air entrainment, in: SFPE Handbook of Fire Protection Engineering. Springer, pp. 396–428.
Heskestad, G., Delichatsios, M.A., 1979. The initial convective flow in fire. Symposium on Combustion 17, 1113–1123.
Hinkley, P.L., 1970. The flow of hot gases along an enclosed shopping mall a tentative theory. Fire Research Notes 807.
Hodges, J.L., 2018. Predicting Large Domain Multi-Physics Fire Behavior Using Artificial Neural Networks. Virginia Polytechnic Institute and State University.
Hodges, J.L., Lattimer, B.Y., Luxbacher, K.D., 2019. Compartment fire predictions using transpose convolutional neural networks. Fire Safety Journal 108, 102854. https://doi.org/10.1016/j.firesaf.2019.102854
Hu, L.H., Chen, L.F., Wu, L., Li, Y.F., Zhang, J.Y., Meng, N., 2013. An experimental investigation and correlation on buoyant gas temperature below ceiling in a slopping tunnel fi re. Applied Thermal Engineering 51, 246–254. https://doi.org/10.1016/j.applthermaleng.2012.07.043
Hu, L.H., Huo, R., Chow, W.K., 2008. Studies on buoyancy-driven back-layering flow in tunnel fires. Experimental Thermal and Fluid Science. https://doi.org/10.1016/j.expthermflusci.2008.03.005
Hu, L.H., Huo, R., Peng, W., Chow, W.K., Yang, R.X., 2006. On the maximum smoke temperature under the ceiling in tunnel fires. Tunnelling and Underground Space Technology 21, 650–655. https://doi.org/10.1016/j.tust.2005.10.003
Huang, Y., Li, Y., Dong, B., Li, J., Liang, Q., 2018. Numerical investigation on the maximum ceiling temperature and longitudinal decay in a sealing tunnel fire. Tunnelling and Underground Space Technology 72, 120–130. https://doi.org/10.1016/j.tust.2017.11.021
Huang, Y., Li, Y., Li, Junmei, Li, Jiaxin, Wu, K., Zhu, K., Li, H., 2019a. Experimental investigation on maximum gas temperature beneath the ceiling in a branched tunnel fire. International Journal of Thermal Sciences 145.

https://doi.org/10.1016/j.ijthermalsci.2019.105997
Huang, Y., Li, Yanfeng, Li, Junmei, Dong, B., Bi, Q., Li, Yan, Li, Jiaxin, 2019b. Experimental inverstigation on temperature profile with downstream vehicle in a longitudinally ventilated tunnel. Experimental Thermal and Fluid Science 103, 149–156. https://doi.org/10.1016/j.expthermflusci.2019.01.006
Ingason, H., 2008. Model scale tunnel tests with water spray. Fire Safety Journal 43, 512–528. https://doi.org/10.1016/j.firesaf.2007.12.002
Ingason, H., 2006. A Fire Tests in the Ofenegg-Tunnel in 1965., in: Flammability Testing of Materials Used in Construction, Transport and Mining. Woodhead Publishing, pp. 231–274.
Ingason, H., 2001. An Overview of Vehicle Fires in Tunnels. Boras, Sweden.
Ingason, H., Kumm, M., Nilsson, D., Lonnermark, A., Claesson, A., Li, Y.Z. et al., 2012. The METRO project - Final Report, STUDIES IN SUSTAINABLE TECHNOLOGY. Mälardalen University Press.
Ingason, H., Li, Y.Z., Lönnermark, A., 2015a. Tunnel fire dynamics, Tunnel Fire Dynamics. Springer, London. https://doi.org/10.1007/978-1-4939-2199-7
Ingason, H., Li, Y.Z., Lönnermark, A., 2015b. Runehamar tunnel fire tests. Fire Safety Journal 71, 134–149. https://doi.org/10.1016/j.firesaf.2014.11.015
Ingason, H., Lönnermark, A., 2005. Heat release rates from heavy goods vehicle trailer fires in tunnels. Fire Safety Journal 40, 646–668. https://doi.org/10.1016/j.firesaf.2005.06.002
Ingason, H., Zhen, Y., 2010. Model scale tunnel fire tests with longitudinal ventilation. Fire Safety Journal 45, 371–384. https://doi.org/10.1016/j.firesaf.2010.07.004
Jaafari, A., Zenner, E.K., Panahi, M., Shahabi, H., 2019. Hybrid artificial intelligence models based on a neuro-fuzzy system and metaheuristic optimization algorithms for spatial prediction of wildfire probability. Agricultural and Forest Meteorology 266–267, 198–207. https://doi.org/10.1016/j.agrformet.2018.12.015
Janssens, M., Tran, H.C., 1992. Data Reduction of Room Tests for Zone Model Validation. Journal of Fire Flammability 10, 528–555.
Japan Road Association, 1985. Tunnel Ventilation Design Guidelines. Tokyo.
Jevtić, R.B., Blagojević, M.D.J., 2014. On a linear fire detection using coaxial cables. Thermal Science 18, 603–614. https://doi.org/10.2298/TSCI130211102J
Ji, J, Fan, C.G., Zhong, W., Shen, X.B., Sun, J.H., 2012. Experimental investigation on influence of different transverse fire locations on maximum smoke temperature under the tunnel ceiling. International Journal of Heat and Mass Transfer 55, 4817–4826. https://doi.org/10.1016/j.ijheatmasstransfer.2012.04.052
Ji, J., Fu, Y., Li, K., Sun, J., Fan, C., Shi, W., 2015a. Experimental study on behavior of sidewall fires at varying height in a corridor-like structure. Proceedings of the Combustion Institute 35, 2639–2646. https://doi.org/10.1016/j.proci.2014.06.041
Ji, J., Gao, Z.H., Fan, C.G., Zhong, W., Sun, J.H., 2012. A study of the effect of plug-holing and boundary layer separation on natural ventilation with vertical shaft in urban road tunnel fires. International Journal of Heat and Mass Transfer 55, 6032–6041. https://doi.org/10.1016/j.ijheatmasstransfer.2012.06.014
Ji, J., Wan, H., Li, K., Han, J., Sun, J., 2015b. A numerical study on upstream maximum temperature in inclined urban road tunnel fires. International Journal of Heat and Mass Transfer 88, 516–526. https://doi.org/10.1016/j.ijheatmasstransfer.2015.05.002
Ji, J., Zhong, W., Li, K.Y., Shen, X.B., Zhang, Y., Huo, R., 2011. A simplified calculation method on maximum smoke temperature under the ceiling in subway station fires. Tunnelling and Underground Space Technology 26, 490–496. https://doi.org/10.1016/j.tust.2011.02.001
Jiang, X., Liao, X., Chen, S., Wang, J., Zhang, S., 2018a. An experimental study on plug-holing in tunnel fi re with central smoke extraction. Applied Thermal Engineering 138, 840–848. https://doi.org/10.1016/j.applthermaleng.2018.04.052
Jiang, X., Zhang, H., Jing, A., 2018b. Effect of blockage ratio on critical velocity in tunnel model fire tests. Tunnelling and Underground Space Technology 82, 584–591. https://doi.org/10.1016/j.tust.2018.09.001
Jie, J., Kaiyuan, L., Wei, Z., Ran, H., 2010. Experimental investigation on influence of smoke venting velocity and vent height on mechanical smoke exhaust efficiency. Journal of Hazardous Materials 177, 209–215. https://doi.org/10.1016/j.jhazmat.2009.12.019
Kashef, A., Yuan, Z., Lei, B., 2013. Ceiling temperature distribution and smoke diffusion in tunnel fires with natural ventilation. Fire Safety Journal 62, 249–255. https://doi.org/10.1016/j.firesaf.2013.09.019
Kennedy, W.D., 1976. Subway Environmental Design Handbook. US Dep of Transportation.
Kennedy, W.D., Parsons, B., 1996. Critical velocity: past, present and future. Paper presented in the One Day Seminar of Smoke and Critical Velocity in Tunnels, London.
Kim, N.K., Jeon, K.M., Kim, H.S., 2019. Convolutional Recurrent Neural Network-Based Multiple Microphones. Sensors 19.
Komer, B., Bergstra, J., Eliasmith, C., 2014. Hyperopt-Sklearn: Automatic Hyperparameter Configuration for Scikit-Learn. Proceedings of the 13th Python in Science Conference 32–37. https://doi.org/10.25080/majora-14bd3278-006
Kuesel, T.R., King, E.H., Bickel, J.O., 2012. Tunnel engineering handbook. Springer Science & Business Media.
Kunsch, J.P., 2002. Simple model for control of fire gases in a ventilated tunnel. Fire Safety Journal 37, 67–81.
Kurioka, H., Oka, Y., Satoh, H., Sugawa, O., 2003. Fire properties in near field of square fire source with longitudinal ventilation in tunnels. Fire Safety Journal 38, 319–340. https://doi.org/10.1016/S0379-7112(02)00089-9
Larson, D., Reese, R., Wilmot, E., 1983. Caldecott Tunnel fire thermal environments regulatory considerations and probabilities. Regulatory Considerations and Probabilities. Sandia National Laboratories.

Lattimer, B.Y., Mealy, C., Beitel, J., 2013. Heat Fluxes and Flame Lengths from Fires Under Ceilings. Fire Technology 49, 269–291. https://doi.org/10.1007/s10694-012-0261-1

Lee, B., Han, D., 2007. Real-time fire detection using camera sequence image in tunnel environment. Lecture Notes in Computer Science (including subseries Lecture Notes in Artificial Intelligence and Lecture Notes in Bioinformatics) 4681 LNCS, 1209–1220.

Lee, C. K, Chaiken, R.F., Singer, J.M., 1979. Longitudinal ventilation analysis for the Glenwood canyon tunnels. Combustion Science and Technology 59–72.

Lee, Calvin K, Chaiken, R.F., Singer, J.M., Lee, C.K., Chaiken, R.F., Singer, J.M., 1979. Interaction Between Duct Fires and Ventilation Flow : An Experimental Study. Combustion Science and Technology 20, 59–72. https://doi.org/10.1080/00102207908946897

Lee, S.R., Ryou, H.S., 2005. An Experimental Study of the Effect of the Aspect Ratio on the Critical Velocity in Longitudinal Ventilation Tunnel Fires. Journal of Fire Sciences. https://doi.org/10.1177/0734904105044630

Lee, Y., Tsai, K., 2012. Effect of vehicular blockage on critical ventilation velocity and tunnel fire behavior in longitudinally ventilated tunnels. Fire Safety Journal 53, 35–42. https://doi.org/10.1016/j.firesaf.2012.06.013

Li, J., Liu, J., 2020. Science Mapping of Tunnel Fires: A Scientometric Analysis-Based Study. Fire Technology 56, 2111–2135. https://doi.org/10.1007/s10694-020-00969-z

Li, Q., Tang, Z., Fang, Z., Yuan, J., Wang, J., 2019. Experimental study of the eff ectiveness of a water mist segment system in blocking fire-induced smoke and heat in mid-scale tunnel tests. Tunnelling and Underground Space Technology 88, 237–249. https://doi.org/10.1016/j.tust.2019.03.011

Li, Y.Z., Ingason, H., 2018. Overview of research on fire safety in underground road and railway tunnels. Tunnelling and Underground Space Technology 81, 568–589. https://doi.org/10.1016/j.tust.2018.08.013

Li, Y.Z., Ingason, H., 2017. Effect of cross section on critical velocity in longitudinally ventilated tunnel fires. Fire Safety Journal 91, 303–311. https://doi.org/10.1016/j.firesaf.2017.03.069

Li, Y.Z., Ingason, H., 2013. Model scale tunnel fire tests with automatic sprinkler. Fire Safety Journal. https://doi.org/10.1016/j.firesaf.2013.09.024

Li, Y.Z., Ingason, H., Lönnermark, A., 2012. Numerical simulation of Runehamar tunnel fire tests. na.

Li, Y.Z., Lei, B., Ingason, H., 2011. The maximum temperature of buoyancy-driven smoke flow beneath the ceiling in tunnel fires. Fire Safety Journal. https://doi.org/10.1016/j.firesaf.2011.02.002

Li, Z.Y., Lei, B., Ingason, H., 2010. Study of critical velocity and backlayering length in longitudinally ventilated tunnel fires. Fire Safety Journal 45, 361–370. https://doi.org/10.1016/j.firesaf.2010.07.003

Lin, P., Wang, Z., Wang, K., Gao, D., Shi, J., You, S., Chen, Z., Wang, G., Mei, X., 2019. An experimental study on self-extinction of methanol fi re in tilted tunnel. Tunnelling and Underground Space Technology 91, 102996. https://doi.org/10.1016/j.tust.2019.102996

Liu, C., Zhong, M., Shi, C., Zhang, P., Tian, X., 2017. Temperature profile of fire-induced smoke in node area of a full-scale mine shaft tunnel under natural ventilation. Applied Thermal Engineering 110, 382–389. https://doi.org/10.1016/j.applthermaleng.2016.08.147

Liu, H., Zhu, G., Pan, R., Yu, M., 2020. Experimental investigation of fire temperature distribution and ceiling temperature prediction in closed utility tunnel. Case Studies in Thermal Engineering 14, 100493. https://doi.org/10.1016/j.csite.2019.100493

Lönnermark, A., Ingason, H., 2006. Fire spread and flame length in large-scale tunnel fires. Fire Technology 42, 283–302. https://doi.org/10.1007/s10694-006-7508-7

Mahdevari, S., Torabi, S.R., 2012. Prediction of tunnel convergence using Artificial Neural Networks. Tunnelling and Underground Space Technology 28, 218–228. https://doi.org/10.1016/j.tust.2011.11.002

Mangs, J., Keski-Rahkonen, O., 1994. Characterization of the Fire Behaviour of a Burning Passenger Car. Part II: Parametrization of Measured Rate of Heat Release Curves. Fire Safety Journal 23, 37–49.

Mashimo, H., 1993. State of the road tunnel safety technology in Japan - Ventilation, Lighting, Safety Equipment. Public Works Research Institute, Japan. https://doi.org/10.1016/S0886-7798(02)00017-2

McCaffrey, B., 1979. Purely buoyant diffusion flames: some experimental results, NBSIR 79-1910. National Bureau of Standards. https://doi.org/NBSIR 79-1910

McGrattan, K., Hostikka, S., McDermott, R., Floyd, J., Vanella, M., 2019. Fire Dynamics Simulator User's Guide. NIST Special Publication 1019 Sixth Edition. https://doi.org/10.6028

Meacham, B., Bowen, R., Traw, J., Moore, A., 2005. Performance-based building regulation: Current situation and future needs. Building Research and Information 33, 91–106. https://doi.org/10.1080/0961321042000322780

Meng, N., Wang, Q., Liu, Z., Li, X., Yang, H., 2017. Smoke flow temperature beneath tunnel ceiling for train fire at subway station : Reduced-scale experiments and correlations. Applied Thermal Engineering 115, 995–1003. https://doi.org/10.1016/j.applthermaleng.2017.01.027

Mohd Tohir, M., Spearpoint, M., 2013. Distribution analysis of the fire severity characteristics of single passenger road vehicles using heat release rate data. Fire Science Reviews 2, 5. https://doi.org/10.1186/2193-0414-2-5

Muhammad, K., Ahmad, J., Baik, S.W., 2018. Early fire detection using convolutional neural networks during surveillance for effective disaster management. Neurocomputing 288, 30–42. https://doi.org/10.1016/j.neucom.2017.04.083

Naser, M.Z., 2019. Fire resistance evaluation through artificial intelligence - A case for timber structures. Fire Safety Journal 105, 1–18. https://doi.org/10.1016/j.firesaf.2019.02.002

NFPA 130, 2014. Standard for Fixed Guideway Transit and Passenger Rail Systems 2014 Edition. National Fire Protection

Agency.
Ntzeremes, P., Kirytopoulos, K., 2019. Evaluating the role of risk assessment for road tunnel fire safety: A comparative review within the EU. Journal of Traffic and Transportation Engineering (English Edition) 6, 282–296. https://doi.org/10.1016/j.jtte.2018.10.008
Oka, Y., Atkinson, G.T., 1995. Control of smoke flow in tunnel fires. Fire Safety Journal. https://doi.org/10.1016/0379-7112(96)00007-0
Oka, Y., Imazeki, O., 2014a. Temperature and velocity distributions of a ceiling jet along an inclined ceiling - Part 1: Approximation with exponential function. Fire Safety Journal 65, 41–52. https://doi.org/10.1016/j.firesaf.2013.07.009
Oka, Y., Imazeki, O., 2014b. Temperature and velocity distributions of a ceiling jet along an inclined ceiling — Part 2 : Approximation based on cubic function and coordinate transformation. Fire Safety Journal 65, 53–61. https://doi.org/10.1016/j.firesaf.2014.02.006
Oka, Y., Imazeki, O., Sugawa, O., 2010. Temperature profile of ceiling jet flow along an inclined unconfined ceiling. Fire Safety Journal 45, 221–227. https://doi.org/10.1016/j.firesaf.2010.03.003
Okamoto, K., Watanabe, N., Hagimoto, Y., Chigira, T., Masano, R., Miura, H., Ochiai, S., Satoh, H., Tamura, Y., Hayano, K., Maeda, Y., Suzuki, J., 2009. Burning behavior of sedan passenger cars. Fire Safety Journal 44, 301–310. https://doi.org/10.1016/j.firesaf.2008.07.001
Ole, S., Cruthers, H.G., 1947. Traffic tunnel and method of tunnel ventilation.
Park, Y., Ryu, J., Ryou, H.S., 2019. Experimental study on the fire-spreading characteristics and heat release rates of burning vehicles using a large-scale calorimeter. Energies 12. https://doi.org/10.3390/en12081465
Pei, G.H., Zhang, Q.Y., 2019. Review of Research on critical velocity in tunnel fire. E3S Web of Conferences 79, 1–4. https://doi.org/10.1051/e3sconf/20197902001
Qiu, A., Hu, L., Chen, L.F., Carvel, R.O., 2018. Flame extension lengths beneath a confined ceiling induced by fire in a channel with longitudinal air flow. Fire Safety Journal 97, 29–43. https://doi.org/10.1016/j.firesaf.2018.02.003
Quintiere, J.G., 2020. Scaling realistic fire scenarios. Progress in Scale Modeling, an International Journal 1, 1–19. https://doi.org/10.13023/psmij.2020.02
Quintiere, J.G., 1989. Scaling Applications in Fire Research * 15, 3–29.
Ren, R., Zhou, H., Hu, Z., He, S., Wang, X., 2019. Statistical analysis of fire accidents in Chinese highway tunnels 2000–2016. Tunnelling and Underground Space Technology 83, 452–460. https://doi.org/10.1016/j.tust.2018.10.008
Rew, W., Deaves, D., 1999. Fire spread and flame length in ventilated tunnels- a model used in Channel tunnel assessment. Fire spread and flame length in ventilated tunnels - a model used in Channel tunnel assessments. Proceedings of the International Conference on Tunnel Fires and Escape from Tunnels. Independent Technical Conferences Ltd., Lyon,.
Roh, J.S., Yang, S.S., Ryou, H.S., Yoon, M.O., Jeong, Y.T., 2008. An experimental study on the effect of ventilation velocity on burning rate in tunnel fires — heptane pool fire case. Building and Environment 43, 1225–1231. https://doi.org/10.1016/j.buildenv.2007.03.007
Russell, S.J., Norvig, P., 2016. Artificial Intelligence: A Modern Approach. Peason Education Limited, Malaysia.
Sarvari, A., Mazinani, S.M., 2019. A new tunnel fire detection and suppression system based on camera image processing and water mist jet fans. Heliyon 5, e01879. https://doi.org/10.1016/j.heliyon.2019.e01879
Sevcik, E.M., 1928. The Holland Vehicular Tunnel: A Great Engineering Achievement.
Shafee, S., Yozgatligil, A., 2018. An experimental study on the burning rates of interacting fires in tunnels. Fire Safety Journal 96, 115–123. https://doi.org/10.1016/j.firesaf.2018.01.004
Shipp, M., Spearpoint, M., 1995. Measurements of the severity of fires involving private motor vehicles. Fire and Materials. https://doi.org/10.1002/fam.810190307
Singh, M., Khurana, S., 2019. Impact of passive fi re protection on heat release rates in road tunnel fi re : A review. Tunnelling and Underground Space Technology 85, 149–159. https://doi.org/10.1016/j.tust.2018.12.018
Spratt, D., Heselden, A.J.M., 1974. Fire Research Note No1001. Fire Research Note, No1001.
Steinert, C., 1994. Smoke and Heat Production in Tunnel Fires, in: The International Conference on Fires in Tunnels, Borås, Sweden, 10–11 October. SP Swedish National Testing and Research Institute, pp. 123–137.
Steward, F.R., 1970. Prediction of the Height of Turbulent Diffusion Buoyant Flames. Combustion Science and Technology 2, 203–212. https://doi.org/10.1080/00102207008952248
Sun, J., Fang, Z., Tang, Z., Beji, T., Merci, B., 2016. Experimental study of the effectiveness of a water system in blocking fire-induced smoke and heat in reduced-scale tunnel tests. Tunnelling and Underground Space Technology incorporating Trenchless Technology Research 56, 34–44. https://doi.org/10.1016/j.tust.2016.02.005
Sun, P., Bisschop, R., Niu, H., Huang, X., 2020. A Review of Battery Fires in Electric Vehicles. Fire Technology 10694. https://doi.org/10.1007/s10694-019-00944-3
Takeuchi, S., Aoki, T., Tanaka, F., Moinuddin, K.A.M., 2017. Modeling for predicting the temperature distribution of smoke during a fire in an underground road tunnel with vertical shafts. Fire Safety Journal 91, 312–319. https://doi.org/10.1016/j.firesaf.2017.03.063
Tanaka, F., Majima, S., Kato, M., Kawabata, N., 2015. Performance validation of a hybrid ventilation strategy comprising longitudinal and point ventilation by a fire experiment using a Smoke diffusion Fire Longitudinal ventilation Transverse ventilation Fire Point ventilation Fire Longitudinal ventilation. Fire Safety Journal 71, 287–298. https://doi.org/10.1016/j.firesaf.2014.11.025
Tanaka, F., Takezawa, K., Hashimoto, Y., Moinuddin, K.A.M., 2018. Critical velocity and backlayering distance in tunnel fires with longitudinal ventilation taking thermal properties of wall materials into consideration. Tunnelling and Underground

Space Technology 75, 36–42. https://doi.org/10.1016/j.tust.2017.12.020

Tang, F., Cao, Z., Palacios, A., Wang, Q., 2018a. A study on the maximum temperature of ceiling jet induced by rectangular-source fires in a tunnel using ceiling smoke extraction. International Journal of Thermal Sciences 127, 329–334. https://doi.org/10.1016/j.ijthermalsci.2018.02.001

Tang, F., He, Q., Chen, L., Li, P., 2019. Experimental study on maximum smoke temperature beneath the ceiling induced by carriage fi re in a tunnel with ceiling smoke extraction. Sustainable Cities and Society 44, 40–45. https://doi.org/10.1016/j.scs.2018.09.026

Tang, F., He, Q., Mei, F., Wang, Q., Zhang, H., 2018b. Effect of ceiling centralized mechanical smoke exhaust on the critical velocity that inhibits the reverse flow of thermal plume in a longitudinal ventilated tunnel. Tunnelling and Underground Space Technology 82, 191–198. https://doi.org/10.1016/j.tust.2018.08.039

Tang, Fei, He, Q., Shi, Q., 2017a. Experimental study on thermal smoke layer thickness with various upstream blockage–fire distances in a longitudinal ventilated tunnel. Journal of Wind Engineering and Industrial Aerodynamics 170, 141–148. https://doi.org/10.1016/j.jweia.2017.08.003

Tang, F., Hu, P., Wen, J., 2020. Experimental investigation on lateral ceiling temperature distribution induced by wall-attached fire with various burner aspect ratios in underground space. Fire Safety Journal 103055. https://doi.org/10.1016/j.firesaf.2020.103055

Tang, Fei, Li, L., Chen, W., Tao, C., Zhan, Z., 2017b. Studies on ceiling maximum thermal smoke temperature and longitudinal decay in a tunnel fire with different transverse gas burner locations. Applied Thermal Engineering 110, 1674–1681. https://doi.org/10.1016/j.applthermaleng.2016.09.054

Tang, F., Li, L.J., Mei, F.Z., Dong, M.S., 2016. Thermal smoke back-layering flow length with ceiling extraction at upstream side of fire source in a longitudinal ventilated tunnel. Applied Thermal Engineering. https://doi.org/10.1016/j.applthermaleng.2016.05.173

Tang, F., Mei, F.Z., Wang, Q., He, Z., Fan, C.G., Tao, C.F., 2017. Maximum temperature beneath the ceiling in tunnel fires with combination of ceiling mechanical smoke extraction and longitudinal ventilation. Tunnelling and Underground Space Technology 68, 231–237. https://doi.org/10.1016/j.tust.2017.05.029

Thomas, P.H., 1968. The movement of smoke in horizontal passages against an air flow. Fire Research Station.

Thomas, P.H., 1963. The size of flames from natural fires. Symposium (International) on Combustion 9, 844–859. https://doi.org/10.1016/S0082-0784(63)80091-0

Thomas, P.H., 1958. The movement of buoyant fluid against a stream and the venting of underground fires. Fire Research Notes.

Thomas, P.H., Webster, C.., Raftery, M.., 1961. Some experiments on buoyant diffusion flames. Combustion and flame 5, 359–367.

Tsai, K., Lee, Y., Lee, S., 2011. Critical ventilation velocity for tunnel fires occurring near tunnel exits. Fire Safety Journal 46, 556–557. https://doi.org/10.1016/j.firesaf.2011.08.003

Ura, F., Kawabata, N., Tanaka, F., 2014. Characteristics of smoke extraction by natural ventilation during a fire in a shallow urban road tunnel with roof openings. Fire Safety Journal 67, 96–106. https://doi.org/10.1016/j.firesaf.2014.05.009

Vantelon, J.P., Guelzim, A., Quach, D., 1991. Investigation of Fire-Induced Smoke Movement in Tunnels and Stations : An Application to the Paris Metro. in: Proceedings of the Third International Symposium on Fire Safety Science, Edinburgh, UK, Elsevier, Oxford, pp. 907–918.

Vauquelin, O., 2005. Parametrical study of the back flow occurrence in case of a buoyant release into a rectangular channel. Experimental Thermal and Fluid Science 29, 725–731. https://doi.org/10.1016/j.expthermflusci.2005.01.002

Vauquelin, O., Telle, D., 2005. Definition and experimental evaluation of the smoke “confinement velocity” in tunnel fires. Fire Safety Journal. https://doi.org/10.1016/j.firesaf.2005.02.004

Vauquelin, O., Wu, Y., 2006. Influence of tunnel width on longitudinal smoke control. Fire Safety Journal 41, 420–426. https://doi.org/10.1016/j.firesaf.2006.02.007

Vianello, C., Fabiano, B., Palazzi, E., Maschio, G., 2012. Experimental study on thermal and toxic hazards connected to fire scenarios in road tunnels. Journal of Loss Prevention in the Process Industries 25, 718–729. https://doi.org/10.1016/j.jlp.2012.04.002

Wan, H., Gao, Z., Ji, J., Li, K., Sun, J., Zhang, Y., 2017. Experimental study on ceiling gas temperature and flame performances of two buoyancy-controlled propane burners located in a tunnel. Applied Energy 185, 573–581. https://doi.org/10.1016/j.apenergy.2016.10.131

Wang, J., Yuan, J., Fang, Z., Tang, Z., Qian, P., Ye, J., 2018. A model for predicting smoke back-layering length in tunnel fi res with the combination of longitudinal ventilation and point extraction ventilation in the roof. Tunnelling and Underground Space Technology 80, 16–25. https://doi.org/10.1016/j.tust.2018.05.022

Wang, Q., Wang, S., Liu, H., Shen, J., Shang, F., Shi, C., Tang, F., 2020. Characterization of ceiling smoke temperature profile and maximum temperature rise induced by double fires in a natural ventilation tunnel. Tunnelling and Underground Space Technology 96, 103233. https://doi.org/10.1016/j.tust.2019.103233

Wang, Y.F., Li, Y.L., Yan, P.N., Zhang, B., Jiang, J. cheng, Zhang, L., 2015. Maximum temperature of smoke beneath ceiling in tunnel fire with vertical shafts. Tunnelling and Underground Space Technology incorporating Trenchless Technology Research 50, 189–198. https://doi.org/10.1016/j.tust.2015.06.011

Wang, Y.F., Qin, T., Sun, X.F., Lui, S., Jiang, J.C., 2016. Full-scale fire experiments and simulation of tunnel with vertical shafts. Applied Thermal Engineering 105, 243–255. https://doi.org/10.1016/j.applthermaleng.2016.05.153

Węgrzyński, W., Lipecki, T., 2018. Wind and Fire Coupled Modelling—Part I: Literature Review. Fire Technology 54, 1405–

1442. https://doi.org/10.1007/s10694-018-0748-5

Weng, M. cheng, Lu, X. ling, Liu, F., Shi, X. peng, Yu, L. xing, 2015. Prediction of backlayering length and critical velocity in metro tunnel fires. Tunnelling and Underground Space Technology. https://doi.org/10.1016/j.tust.2014.12.010

Wu, F., Zhou, R., Shen, G., Jiang, J., Li, K., 2018. Effects of ambient pressure on smoke back-layering in subway tunnel fires. Tunnelling and Underground Space Technology 79, 134–142. https://doi.org/10.1016/j.tust.2018.05.011

Wu, X., Park, Y., Li, A., Huang, X., Xiao, F., Usmani, A., 2020a. Smart Detection of Fire Source in Tunnel Based on the Numerical Database and Artificial Intelligence. Fire Technology. https://doi.org/10.1007/s10694-020-00985-z

Wu, X., Zhang, X., Huang, X., Xiao, F., Usmani, A., 2020b. A Real-time Fire Forecast in Tunnel Based on Big Data and Artificial Intelligence. Tunnelling and Underground Space Technology [under review].

Wu, Y., Bakar, M.Z.A., 2000. Control of smoke flow in tunnel fires using longitudinal ventilation systems - a study of the critical velocity. Fire Safety Journal. https://doi.org/10.1016/S0379-7112(00)00031-X

Xu, Z., Zhao, J., Liu, Q., Chen, H., Liu, Y., Geng, Z., He, L., 2019. Experimental investigation on smoke spread characteristics and smoke layer height in tunnels. Fire and Materials. https://doi.org/10.1002/fam.2701

Xue, C.J., 2010. The road tunnel fire detection of multi-parameters based on BP neural network. CAR 2010 - 2010 2nd International Asia Conference on Informatics in Control, Automation and Robotics 3, 246–249. https://doi.org/10.1109/CAR.2010.5456677

Yao, Y., He, K., Peng, M., Shi, L., Cheng, X., Zhang, H., 2018. Maximum gas temperature rise beneath the ceiling in a portals-sealed tunnel fire. Tunnelling and Underground Space Technology 80, 10–15. https://doi.org/10.1016/j.tust.2018.05.021

Yao, Y., Li, Y.Z., Lönnermark, A., Ingason, H., Cheng, X., 2019. Study of tunnel fires during construction using a model scale tunnel. Tunnelling and Underground Space Technology 89, 50–67. https://doi.org/10.1016/j.tust.2019.03.017

Yi, L., Xu, Q., Xu, Z., Wu, D., 2014. An experimental study on critical velocity in sloping tunnel with longitudinal ventilation under fire. Tunnelling and Underground Space Technology 43, 198–203. https://doi.org/10.1016/j.tust.2014.05.017

You, H.Z., Faeth, G.M., 1979. Ceiling heat transfer during fire plume and fire impingement. Fire and Materials 3, 140–147. https://doi.org/10.1002/fam.810030305

Yu, L., Liu, F., Liu, Y., Weng, M., Liao, S., 2018. Experimental study on thermal and smoke control using transverse ventilation in a sloping urban traffic link tunnel fire. Tunnelling and Underground Space Technology 71, 81–93. https://doi.org/10.1016/j.tust.2017.08.012

Zhang, S., Cheng, X., Yao, Y., Zhu, K., Li, K., Lu, S., Zhang, R., Zhang, H., 2016. An experimental investigation on blockage effect of metro train on the smoke back-layering in subway tunnel fires. Applied Thermal Engineering 99, 214–223. https://doi.org/10.1016/j.applthermaleng.2015.12.085

Zhang, X., Xu, Z., Ni, T., Peng, J., Zeng, J., 2019. Investigation on smoke temperature distribution in a double-deck tunnel fire with longitudinal ventilation and lateral smoke extraction. Case Studies in Thermal Engineering 13, 100375. https://doi.org/10.1016/j.csite.2018.100375

Zhang, Xiaochun, Hu, L., Zhu, W., Zhang, Xiaolei, Yang, L., 2014. Flame extension length and temperature profile in thermal impinging flow of buoyant round jet upon a horizontal plate. Applied Thermal Engineering 73, 15–22. https://doi.org/10.1016/j.applthermaleng.2014.07.016

Zhang, Xiaochun, Tao, H., Xu, W., Liu, X., Li, X., Zhang, Xiaolei, Hu, L., 2017. Flame extension lengths beneath an inclined ceiling induced by rectangular-source fires. Combustion and Flame 176, 349–357. https://doi.org/10.1016/j.combustflame.2016.11.004

Zhao, S., Liu, F., Wang, F., Weng, M., 2018. Experimental studies on fi re-induced temperature distribution below ceiling in a longitudinal ventilated metro tunnel. Tunnelling and Underground Space Technology 72, 281–293. https://doi.org/10.1016/j.tust.2017.11.032

Zhen, Y., Ingason, H., 2012. The maximum ceiling gas temperature in a large tunnel fire. Fire Safety Journal 48, 38–48. https://doi.org/10.1016/j.firesaf.2011.12.011

Zhou, T., He, Y., Lin, X., Wang, X., Wang, J., 2017a. Influence of constraint effect of sidewall on maximum smoke temperature distribution under a tunnel ceiling. Applied Thermal Engineering 112, 932–941. https://doi.org/10.1016/j.applthermaleng.2016.10.111

Zhou, T., Liu, J., Chen, Q., Chen, X., Wang, J., 2017b. Characteristics of smoke movement with forced ventilation by movable fan in a tunnel fire. Tunnelling and Underground Space Technology incorporating Trenchless Technology Research 64, 95–102. https://doi.org/10.1016/j.tust.2017.01.013

Zhou, T., Wang, X., He, J., Chen, Q., Wang, J., 2019. The effect of forced ventilation by using two movable fans on thermal smoke movement in a tunnel fire. Journal of Wind Engineering & Industrial Aerodynamics 184, 321–328. https://doi.org/10.1016/j.jweia.2018.12.003

Zinoubi, J., Ben, R., 2019. International Journal of Thermal Sciences Numerical study on the thermal buoyant flow stratification in tunnel fires with longitudinal imposed air flow : Effect of an upstream blockage. International Journal of Thermal Sciences 136, 230–242. https://doi.org/10.1016/j.ijthermalsci.2018.10.041